Defining mRNA vaccine-generated T cell memory in respiratory viral infection

Kurt B. Pruner

A dissertation

submitted in partial fulfillment of the

requirements for the degree of

Doctor of Philosophy

University of Washington

2024

Reading Committee:

Marion Pepper, Chair

Neil King

Daniel J. Campbell

Program authorized to offer degree:

Department of Immunology

University of Washington

Abstract

Defining mRNA vaccine-generated T cell memory in respiratory viral infection

Kurt B. Pruner

Chair of the Supervisory Committee:

Marion Pepper

Department of Immunology

T cell immune memory provides protective effector mechanisms to restrict pathogen growth upon secondary infection, although the ability of T cells generated by novel mRNA-LNP vaccines to restrict viral infection in currently unknown. To address this, we studied antigen-specific T cell memory generated by mRNA-LNP vaccines in both humans and mice. We report that functional and durable T cell memory is induced by mRNA vaccines in humans, and we define functional T cell correlates of so-called ‘hybrid immunity’ through the study of T cell cytokine production in human blood. Further, we report that mRNA-LNP immunization of mice provides incomplete benefits when compared to previous infection and unexposed naïve mice challenged with influenza virus in the absence of neutralizing antibodies. This intermediate state of protection was associated with a lack of resident memory cells following initial vaccination but expeditated T cell recruitment and adaptation to the lung when compared to unexposed mice. Together, our data imply that mRNA-LNP vaccine-generated memory T cells can provide limited protective capacity in the absence of neutralizing antibodies, but this protective benefit could be substantially improved by adapting aspects of previous infection in future vaccine regimens.

Table of Contents

List of Figures

Dedication

I would like to dedicate this academic work to my mother, Kimberly, for without her, my journey into science would not have been made a reality.

Acknowledgements

I would first like to acknowledge my mentor, Dr. Marion Pepper, for her invaluable scientific advice, direction, and teaching throughout my academic work in her lab. On a different note, I would like to also thank and acknowledge her for the immense and continued attention, passion, and genuine care I felt toward her investment in my mental health, career development, and scientific fulfillment even during stressful and transitionary periods of her career and through a global pandemic. I will be forever grateful for my time working with you. Thank you.

I would also like to thank my scientific colleagues in the Pepper Lab and the Department of Immunology, especially those involved in the COVID-19 collaborative studies. Working alongside each of you has held me to a higher standard of science and this is an inditement to all your academic and scientific rigor. In addition, I am thankful for the generous collaborations I have been able to participate in, namely with the lab of Drew Weissman at University of Pennsylvania who provided the LNP-mRNA-NP vaccine constructs for our animal studies.

I would like to acknowledge my classmates at the University of Washington for your friendship and comradery through the first few years of transition to Seattle. I would also like to acknowledge my friends in Seattle and Boston who have been there often to keep my spirits high and guide me through difficult times in the trek which is graduate school. This experience would have been painstaking and gruesome if not for the patches of light you so often interjected into my day-to-day life.

Finally, I would like to thank my family who have always stressed the importance of education, knowledge, and discovery. Particularly my parents Ken and Kim, who were my honest best friends during the first year in Seattle. Finally, I would be remiss if I did not thank my partner Kennidy, who has been there for me in all hours of the day, talking through my science, giving me pep talks, holding me to the highest standards, and spending some of the best memories I have in the past years, together. Thank you all, so much.

1 Introduction

1.1 The generation of antigen-restricted T cell memory

T cells and B cells of the adaptive immune system have evolved to recognize foreign antigens in a highly specific manner, allowing for a tightly regulated immune response to previously encountered pathogens. To do this, each T cell undergoes stochastic recombination of its antigen-reactive T cell receptor (TCR) in the thymus, thereby creating an immensely diverse pool of recirculating naïve T cells. Therefore, as a population, the T cell repertoire has the potential to react to effectively every foreign protein introduced to the organism. TCR sequencing approaches have estimated that the naive repertoire of a mouse consists of 2×10^6 clones, each expressing a unique TCR [1]. Although such a diverse repertoire is necessary to recognize and protect against the vast array of pathogens an organism may encounter, it also presents the immune system with a challenge: Very small populations of T cells must expand, functionally differentiate, and disperse throughout the body to effectively clear a pathogen.

T cell activation is initiated when a TCR recognizes a specific peptide presented on class II major histocompatibility complexes (MHC-II) expressed by antigen-presenting cells (APCs) [2]. Inputs integrated from TCR binding, signaling downstream of costimulatory molecules, and innate cell–derived cytokines are incorporated into transcriptional networks that direct the expansion, gain of effector function, and migration of a responding naive cell. For example, in an T helper type 1 (Th1) response to an invading virus, a virus-specific T cell population can expand from several hundred to several hundred thousand cells, gain the ability to express a variety of antiviral cytokines (e.g., IFN-γ, IL-2, TNF, and IL-10) or killing programs, and migrate to various tissues to activate downstream target cells and effectively clear virus.

Upon the clearance of pathogen and during the resolution of inflammation, approximately 90% activated effector T cells undergo apoptosis in a process referred to as T cell contraction [3]. The cells which remain are memory T cells and persist through perception of the pro-survival

cytokines IL-7 and IL-15 for the remainder of life. At least three distinct subsets of memory T cells have been described: $CD62L^+$ central memory T (Tcm) cells, $CD62L^-$ effector memory T (Tem) cells, and $CD62L^-CD69^+$ tissue-resident memory T (Trm) cells [4]. Tcm and Tem cells patrol the spleen/lymph nodes and recirculate in the peripheral blood, respectively, whereas Trm cells undergo contraction while localized in nonlymphoid barrier tissues and continuously patrol extravascular niches in organs such as the skin, lung, intestine, or reproductive tract. Together, this antigen-specific T cell compartment can survey all pertinent sites of pathogen invasion and act in concert to rapidly clear secondary infection in a highly specific and regulated manner.

The divergent localization of memory T cell subsets is reflected in their distinct reactivation dynamics. Tcm cells, located in secondary lymphoid organs (SLO), undergo extensive levels of proliferation, and support the expansion of an abundant antigen-specific T cell compartment upon reactivation. Tem cells have less proliferative potential but can quickly enter sites of infection and/or barrier tissues due to their maintenance in the circulation [4]. Trm cells are often the first to detect an instance of secondary reinfection, due to their proximity to pathogen entry, and can rapidly secrete cytokines and effector molecules that activate the tissue site and, in some cases, directly clear pathogen to provide protection [5-8]. Because of their activity within major organs, their proven effectiveness at clearing pathogens, and their relatively recent discovery, understanding the generation, maintenance, and effector programs of Trm cells represents an important area of investigation for the inception of next-generation vaccines and therapeutics.

1.2 Virus-specific T cell memory in the respiratory tract

Virus-specific memory T cells can behave as sentinels against reinfection due to their localization. Memory T cells persist in various anatomical compartments following respiratory viral infection, including the blood, lymphatic organs, and lungs [9-10]. Multiple studies have focused on the ability of Trm to facilitate an optimally efficient response to viral reinfection, and they have

therefore become an important focus of investigation. Using parabiosis experiments in mice, virus-specific CD4 and CD8 Trm cells have been observed to be retained in tissues across the body following systemic and mucosal viral infections [11-12]. Following *in vivo* antigen restimulation, both CD4 and CD8 T_{rm} cells can rapidly secrete cytokines, including IFN-γ, which facilitates the recruitment of circulating immune cells and the activation of other resident cells critical for protection against disease [12-13]. For example, in two separate animal models, the activation of viral-specific CD8 and CD4 T_{rm} cells was required to control viral burden during reinfection in the skin and female reproductive tract through the production of IFN-γ [13-14]. In studies focused on respiratory infection, the transfer of CD4 lung Trm cells from mice that had previously cleared influenza virus protected unexposed mice from infection, while the transfer of spleen-derived memory T cells provided no better protection than naive T cells [15]. This inability of circulating T cell memory to recapitulate the protection afforded by aspects of resident memory has been reported frequently [16-18] and highlights the importance of understanding Trm cell biology for protection against viral infections.

Trm cells act as sentinels that prevent respiratory disease through their ability to localize to tissues, reactivate in response to reinfection, and rapidly express effector molecules to limit viral replication. Although naive and resting memory T cells share the expression of ~95% of their transcriptome, memory T cells selectively possess an epigenetic landscape that retains open accessibility to genes that were expressed during their effector phase [19-20]. Demethylated chromatin at sites of effector genes, such as CXCR3, CXCR5, CCR5, IL-2Rα, IL-18Rα, IFN-γ, granzyme B, and perforin, have been detected in memory T cells, allowing for rapid transcription and accelerated effector protein production in response to TCR stimulation [19, 21]. Using in vitro ovalbumin peptide simulations, ovalbumin-specific CD4 memory T cells have been shown to display an open chromatin landscape at the IFNG locus, allowing for rapid production of IFN-γ within 2 h [22]. In stark contrast, a naive ovalbumin-specific CD4 T cell migrating through lymphoid organs must find an APC expressing its pMHCII in the context of costimulation and cytokines,

which would lead to the upregulation of T-bet, bearing a delay of up to 24 h before it gained the ability to open the IFNG locus [22]. Additionally, in response to ex vivo restimulation, CD4 Trm cells isolated from human airways produced the effector cytokines IFN-γ and TNF-α faster and in larger quantities compared with circulating CD4 memory cells from the blood, suggesting that Trm cells represent the memory T cell compartment that is the most epigenetically poised to respond rapidly to viral reinfection [23].

Cytokines produced rapidly by memory CD4 Trm cells are essential for the accelerated recruitment, localization, and activation of innate immune cells only hours after reinfection, a process that takes up to 1 d in mice without CD4 Trm cells [24]. In a model of secondary influenza infection, upregulation of the secondary effector molecules IL-1α, IL-1β, TNF-α, IL-6, and the chemokines CXCL9, CXCL10, and CCL2 by tissue-residing innate cells depended on the presence of CD4 Trm cells and their interactions with $CD11c^+$ cells presenting viral antigen on pMHCII [24-25]. In these settings, innate cells also facilitated the recruitment of $Ly6C^+$ monocytes from the bloodstream to further amplify rapid antiviral activity [24]. Importantly, through their immediate production of IFN-γ, CD4 Trm cells can modulate the localization of key effector cells to sites of active viral replication in the respiratory tract. Since most respiratory viruses propagate by infecting cells within the airways and not the parenchyma, many viral-specific CD4 Trm cells constitutively express the chemokine receptor CXCR3 and integrin CD49a (VLA-1) and can rapidly migrate to subepithelial or bronchoalveolar spaces in response to the CXCR3 ligands CXCL9 and CXCL10 produced by infected airway epithelial cells [26-28]. Unlike what is seen in certain bacterial infections like *Mycobacterium tuberculosis* [29], viral-specific CD4 T cells localized to the airways produce the largest amount of cytokines, including IFN-γ, IL-10, and IL-2. In a model of SARS-CoV-1 vaccination, the blockade of IFN-γ either by administration of IFN-γ–blocking antibody or depletion of CD4 Trm cells in the airway led to a loss in protection from viral challenge [30]. In this study, it was determined that IFN-γ from CD4 Trm cells was needed

to activate resident dendritic cells (DCs) and recruit CXCR3$^+$ memory CD8 Trm cells to the airway through the IFN-γ–dependent upregulation of CXCL9 and CXCL10. Notably, only the blockade of IFN-γ during a secondary, but not a primary, infection with influenza restricted viral clearance [18], underscoring its select role in secondary responses.

In addition to IFN-γ, CD4 Trm cells can also rapidly produce the cytokines TNF-α and IL-10, although these cytokines have been shown to be either beneficial or detrimental to the host depending on the model of infection studied. In a model of respiratory syncytial virus (RSV) infection, mice that received TNF-α–blocking antibodies developed reduced tissue pathology and clinical disease. In this study, mice treated with anti–TNF-α also produced lower levels of IFN-γ from their CD4 T cell compartment, suggesting that TNF-α production may cause T cell–dependent pathology in the lung [31]. Conversely, TNF-α KO mice during primary influenza infection displayed reduced viral burden and weight loss and heightened levels of both IFN-γ–producing virus-specific CD8 T cells in the lungs and hemagglutinin (HA)-specific antibody in the serum, suggesting that TNF-α production was suppressing a productive adaptive immune response [32]. Additionally, in coronavirus infection, the i.n. administration of recombinant TNF-α to naive mice 12 h before challenge with SARS-CoV led to decreased survival [30]. These conflicting reports and the relatively small body of detailed research on the mechanism of TNF-α during viral infection highlights the need to study this important cytokine, especially as it is often used as a proxy of productive antiviral immunity, and its blockade is a common therapy for diseases such as rheumatoid arthritis and inflammatory bowel disease.

IL-10, a key regulatory cytokine in the lung, has been shown to be produced by T-bet$^+$ FOXP3$^-$ effector [33] and memory [30] CD4 T cells in the lung. To prevent lethal immunopathology during the late stages of influenza infection, CD4 T cells are required to orchestrate a contraction of the inflammatory immune response through the upregulation of IL-10 in activated effector T cells [34-35]. Although necessary for restraining lethal inflammation, IL-10 has also been shown

to diminish the antibody response to influenza virus [34], and its deletion led to survival in a model of lethal influenza infection [36]. Therefore, as is likely the case for TNFα, the role of IL-10 and the relative production of IL-10 by CD4 Trm may vary depending on the timing, nature, and severity of the infection. For example, compared to a primary response, lower levels of IL-10 are produced during the secondary response to influenza infection [37]. This phenomenon is likely explained by the accelerated antiviral response to secondary infection when local T cell memory is present. Since viral burden is kept in check, the immune system does not employ a highly inflammatory response to clear infection and perhaps does not need large quantities of anti-inflammatory mediators such as IL-10 to dampen inflammation.

In addition to cytokine production, some CD4 T cells have been shown to engage in pMHCII-restricted lysis of virus-infected cells, a mechanism of viral control previously thought to be restricted to CD8 cytotoxic lymphocytes (CTLs) [38]. CD4 CTLs have been described clustered around infected cells in the airways and produce the effector molecules granzyme-B and perforin [39]. CD4 CTLs are dependent on IL-2, Blimp-1, and Eomes for their generation [40], as well as type-I interferon [41], which is produced by infected airway epithelial cells [42]. Intriguingly, CD4 T cell differentiation to a CD8 CTL-like fate is mediated by repression of the transcription factor ThPOK [43], which alternatively is needed to repress CD8-associated molecules in thymic and peripheral differentiation of CD4 T cells [44-45]. More research is needed to determine the fate of these cells following viral clearance as Trm are not detected in the airways at memory timepoints [46], and ThPOK is necessary for the generation of functional central memory CD4 T cells and their production of IL-2 [47].

Although many virus-specific CD4 Trm migrate to the airways to combat active viral replication [30], there is also a functionally distinct population of CD4 Trm which remain in the parenchymal lung tissue and provide important helper functions to other virus-specific immune cells. Following contraction of a primary immune response, two distinct populations of CD4 Trm form in the lung that can be detected by their reciprocal expression of folate receptor 4 (FR4) and

P-selectin glycoprotein ligand 1 (PSGL1) [48-49]. $PSGL1^{+}FR4^{-}$ CD4 Trm express higher levels of T-bet and CXCR6, resembling a sentinel CD4 Trm subset that rapidly migrates to areas of infection and engages in direct viral clearance. In contrast, $FR4^{+}PSGL1^{-}$ CD4 Trm selectively express PD-1, CXCR5, CXCR4, and ICOS, depend on BCL-6, MHC-II, and B cells for their development, and co-localize with B cells within the parenchymal lung tissue [48-49]. During influenza reinfection, mice that did not develop CD4 Trm with the capability to cluster with B cells had an inability to produce large amounts of HA- or NP-specific B cells or antibodies and displayed reduced survival [49].

The clustering of CD4 Trm with other immune cells, including B cells, $CD21^{+}$ follicular DCs, and CD8 T cells, in peri-bronchial areas of the lung was previously described and is sometimes referred to as inducible bronchus-associated lymphoid tissue (iBALT) [50]. iBALT has been shown to have direct access to inhaled antigen through specialized M cells [51], and provides a niche for adaptive immune cells to interact and proliferate in response to infection, suggesting an advantageous role as a local lymphatic compartment that can provide the functions of a traditional lymphoid organ while being located at the site of infection. Although iBALT can form independently of lymphoid tissue inducer cells necessary for development of lymphoid organs, iBALT formation does require the upregulation of CXCL13 and CCL19, which are important mediators of lymphoid architecture, by stromal cells and DCs [52]. In a model of influenza infection, the release of type-1 interferon drove the production of CXCL13 by lung fibroblasts and facilitated recruitment of $CXCR5^{+}$ B cells to the lung parenchyma, which were necessary for iBALT formation [53]. Indeed, B cells are active mediators of iBALT functionality, as the depletion of B cells led to a decrease in BCL-6, CXCR5, and ICOS-expressing CD4 Trm and a concomitant decrease in CD8 Trm maintenance and the production of antibody from lung-residing B cells (BRM) during reinfection events [48-49]. Further, respiratory viral infection in **μ**MT mice, which lack B cells, drove more virus-specific T cells to the lung parenchyma during effector phases of the infection but led to reduced numbers of long-lived memory CD4 Trm compared to WT mice,

suggesting that B cells are essential for the survival and maintenance of CD4 Trm in the lung in the memory phase [54]. Therefore, iBALT represents an important niche for the maintenance of virus specific CD4 Trm populations in the lung, as has been shown in ectopic memory lymphocyte clusters in other tissues [14], and in an allergic airway model of pulmonary inflammation [55]. Upon reactivation in iBALT, CD4 Trm have been shown to co-localize with Brm, providing a rapid burst of virus-specific antibodies from local plasmablasts [48, 56], while also leading to further affinity maturation of lung Brm toward broadly-neutralizing, cross-reactive epitopes that are highly protective in heterologous infections [49, 57-58]. Indeed, CD4 Trm aid in local production of antibodies by Brm in other models of inflammation [59].

In addition to B cells, CD4 Trm have been shown to co-localize with CD8 T cells and conventional DCs in peri-follicular areas of iBALT and to augment CD8 T cell homing and fitness through their production of IFNγ and/or IL-21 during late stages of influenza infection [49, 60-62]. Further, in a model of CD8 Trm reactivation by latent herpes simplex virus infection, signals from CD4 T cells in the tissue were shown to be essential for the expansion of virus-specific CD8 Trm through a tripartite interaction involving recruited monocyte-derived dendritic cells [63]. These data further support seminal work which showed impaired virus specific CD8 T cell recall responses in the lymphoid tissue in the absence of CD4 T cells [64]. Interestingly, CD4 T cells are not required for the resurgence of CD8 effector mechanisms such as specific lysis or IFNγ production on a per-cell basis, suggesting that signals from CD4 T cells may selectively modulate the expansion of CD8 T cells, perhaps representing a mechanism to amplify the CD8 secondary effector response depending on viral load or inflammatory cues during reinfection.

As a note, iBALT with organized follicles containing germinal center B cells, CXCR5$^+$ Tfh cells, and CD21$^+$ follicular DCs are not detected in all instances of respiratory virus infection [65]. However, even when iBALT is not present, loose clusters of PD-1$^+$ CD4 T cells and B cells are still detected in the lung parenchymal tissue and these T cells are able to provide help to BRM to induce activation and class-switching to IgA [66]. Further, CD4 Trm in the female reproductive

tract, which does not feature densely organized iBALT-like structures, have been shown to induce an expansion of CD8 CTLs, B cells, and activated $CCR2^+$ and $CCR7^+CD86^+$ DCs in response to secondary stimulation with sterile antigen *in vivo* [12]. Therefore, even in the absence of distinct iBALT structures, helper functions of CD4 T cells persist, although more research is needed to determine the importance of these structures in secondary viral infection.

1.3 Understanding immune memory during the COVID-19 pandemic

Respiratory virus outbreaks have deleteriously impacted global health and prosperity throughout human history. A lack of immunity to emergent respiratory viral infections is the underlying cause of several global pandemics that have occurred over the past century, including influenza A pandemics [67] and novel coronavirus pandemics, such as the current SARS-CoV-2 pandemic responsible for ~ 2.5 million deaths [68]. Although neutralizing antibodies produced by B cells in the bone marrow, called long-lived plasma cells (LLPCs), offer excellent protection to previously circulated strains of respiratory viruses [69], the occasional zoonotic emergence or recombination event results in viral clades with novel surface proteins that are not well-recognized by circulating antibodies or memory lymphocytes, introducing the potential for unrestrained infection or pandemic [70-71]. Even when partial immunity in many communities exists, as seen in the seasonal influenza epidemics, significant mortality and loss of productivity remains [72]. Understanding how to elicit immunity to respiratory viruses through vaccination to prevent the emergence of disease is therefore a significant focus of ongoing research.

The immune system is rapidly called into action if a respiratory virus can productively infect a host. While it takes days to mount a primary adaptive immune response to a previously unperceived virus, memory lymphocytes can become activated in response to a prior or closely related viral infection within hours. Layers of adaptive immune memory have evolved to respond to homologous or heterologous viral antigens through a variety of mechanisms. LLPCs provide the first line of defense by constitutively secreting antibodies. While these antibodies may provide

sterilizing immunity to homologous infection, they also exert immune pressure on viral surface antigens, evolutionarily driving the outgrowth of mutated virions. Cross-reactive memory T and B lymphocytes are therefore an important next layer of protection from viruses that may express closely related surface proteins but have mutated to evade the circulating LLPC-derived antibody repertoire. While some memory B cells can rapidly respond to heterologous reinfection by making antibody secreting cells (ASCs) [73], others can re-enter a germinal center response for further diversification [74-76]. Memory T cells retain the ability to respond to homologous or heterologous viral antigens both through their ability to bind peptide:MHC (pMHC) complexes with a broad range of receptor affinities, as well as through their capacity to respond to intracellular proteins that may have avoided antibody-mediated immune pressure. This is important, as many of the intracellular antigens are critical, highly conserved housekeeping proteins necessary for viral replication and function. For example, memory CD4 and CD8 T cells elicited by seasonal influenza A infection can be rapidly activated *ex vivo* in response to elements of pandemic strains of influenza, including H5N1, H3N2, and H1N1 [77-78], and their presence correlates inversely with disease severity, even in the absence of neutralizing antibodies [79-80]. When analyzed in more detail, T cell cross-reactivity to pandemic strains was heavily enriched for clones specific to the internal proteins NP and M1 [81], supporting the notion that internal proteins are more highly conserved between seasonal and pandemic strains of virus [82].

The rapid spread of the SARS-CoV-2 betacoronavirus has infected and killed millions of people worldwide since 2020. Infection causes the disease COVID-19, which ranges in presentation from asymptomatic to fatal. Community-level immunity, acquired through infection or vaccination, is necessary to control the pandemic as the virus continues to circulate. At the start of the COVID-19 pandemic, it was unclear whether infection with the SARS-CoV-2 virus induced durable and functional immune memory, which would be necessary for protection against bouts of future COVID-19 disease in convalescents. Additionally, due to the rapid implementation of novel SARS-CoV-2 RBD mRNA vaccines, limited data was available on the quantity, durability,

and quality of mRNA-generated immune memory. As the pandemic evolved, SARS-CoV-2 variants of concern (VOC) emerged due to selective pressure against neutralizing antibody epitopes of the SARS-CoV-2 receptor binding domain (RBD). Immune memory-mediated protection against VOC strains differed based on exposure history and relative escape from parent-strain neutralizing antibody epitopes but overall, previous infection or immunization provided superior protection vs. the lack of immune memory. Additionally, so-called ‘‘hybrid immunity’’ induced by a combination of prior SARS-CoV-2 infection and subsequent COVID-19 vaccination provided greater protection against re-infection and severe COVID-19 disease than either infection or vaccination alone [83-87].

Together, the SARS-CoV-2 pandemic necessitated highly efficient and accurate measurement of the SARS-CoV-2-specifc immune compartment to understand the evolving pandemic and inform the implementation of effective interventional strategies, such as vaccines. In addition, the SARS-CoV-2 pandemic created a situation in which nascent memory could be tracked through additional antigen exposures. The site of antigen encounter, specific inflammatory signals, and the number, timing, and frequency of antigen exposures all influence the resulting memory pool, yet the specific rules governing memory formation remain undefined. Understanding how the confluence of these parameters influences immune memory function and maintenance is critical for optimizing protective vaccines.

In summary, much is still to be learned concerning the dynamics and diverse functions of T cell memory during natural viral infection of the respiratory tract. Future research into facets of T cell-mediated protection in natural respiratory infection and the mechanisms in which Trm are generated and involved in viral clearance will provide invaluable information for vaccines designed to elicit local immunity in tissue niches, enabling optimal protection from future global pandemics.

2 Functionally imprinted SARS-CoV-2-specific memory T cells define protective correlates of exposure history in vaccinated and infected humans

2.1 Introduction

The generation of immune memory is influenced by signals that B and T lymphocytes of the adaptive immune system perceive during a primary immune response. This system has evolved such that key cues from an invading pathogen or vaccine are relayed to lymphocytes so that they can provide specific functional outputs to combat infection and protect from re-infection. The site of antigen encounter, specific inflammatory signals, and the number, timing, and frequency of antigen exposures all influence the resulting memory pool, yet the specific rules governing memory formation remain undefined. Understanding how the confluence of these parameters influences immune memory function and maintenance is critical for optimizing protective vaccines.

In the context of the SARS-CoV-2 pandemic, the so-called ‘‘hybrid immunity’’ induced by a combination of prior SARS-CoV-2 infection and subsequent COVID-19 vaccination provides greater protection against re-infection and severe COVID-19 disease than either infection or vaccination alone [83-87]. Studies investigating immune correlates of hybrid immunity have revealed improved breadth and neutralizing ability of circulating antibodies from previously infected (PI) individuals [88-91], but the specific changes in the cellular immune compartment associated with this immune state remain undefined. Additionally, it is not understood whether further activation of immune memory in vaccinated-only individuals could achieve similar qualities, as PI individuals have had an additional antigen exposure.

To answer these questions, we tracked circulating SARS- CoV-2-specific memory lymphocytes in a cohort of naive (N) or SARS-CoV-2-PI subjects over the course of three vaccinations. We focused on visualizing spike (S)-specific $CD4^+$ T cells, as they are critical

mediators of protection in infected individuals over a 2-year period and induced by SARS-CoV-2-directed vaccines [92-95].

We find that the immune memory landscape elicited by vaccination of PI subjects is distinct from the immune memory of SARS-CoV-2-naive individuals. Examination of the T cell compartment revealed that although N and PI individuals generated equivalent numbers of S-specific CD4 T cells after vaccination, there was a profound functional skewing toward a Th1 phenotype in PI subjects. CD4 T cell functional differences between N and PI subjects persisted following the administration of a vaccine booster. Further we observed no increase in memory T cells, indicating that the immune memory compartment is likely maximized after the two-dose regimen. Thus, our data support a model in which the priming environment induced by SARS-CoV-2 infection imprints immune memory with multiple features of enhanced type-1 antiviral immunity. These likely contribute to the increased protection associated with hybrid immunity and are not fully recapitulated by repeat vaccination.

2.2 Results

CD4 T cell responses to vaccination were assessed in N and PI individuals using an activation induced marker (AIM) assay based on expression of CD69 and CD154 to detect SARS-CoV-2 specificity [96] (Figures **1B** and **1C**). PBMCs from N or PI donors isolated before and after vaccination were re-stimulated in the presence of peptide pools optimized for the induction of MHC class II-dependent CD4 T cell responses (15-mers) and containing predicted T cell epitopes across a range of common HLA haplotypes against the viral membrane and nucleocapsid (M/N) or spike (S) proteins.

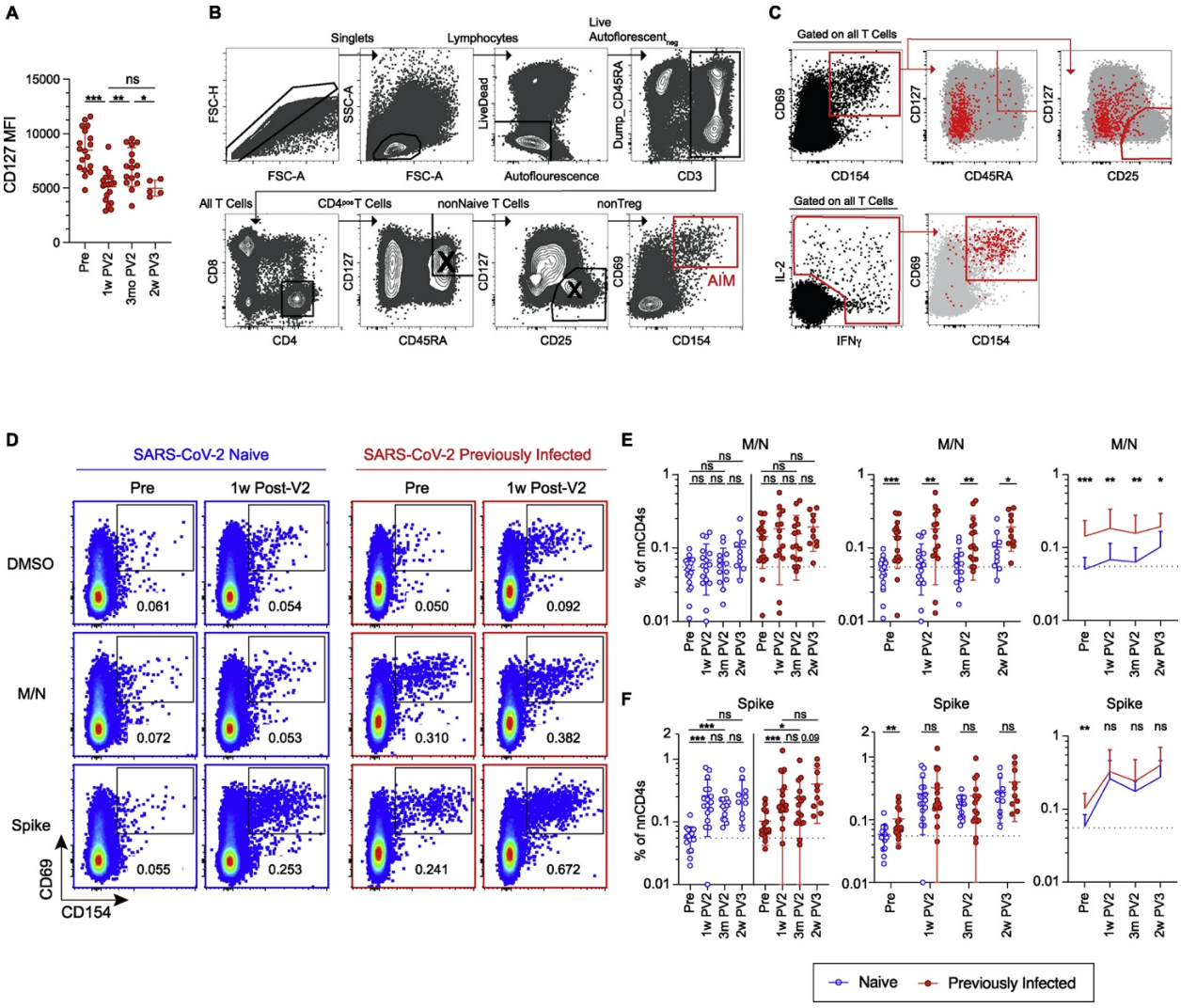

Figure 1: **Robust and durable CD4 T cell responses to SARS-CoV-2 in both previously naive and previously infected individuals.** (A) Mean fluorescent intensity (MFI) of CD127 on AIM CD4$^+$ T cells in previously infected (red) participants. (B) AIM gating strategy depicting removal of naive CD45RA$^+$CD127$^+$ T cells and CD25$^+$CD127$^-$ T regulatory cells. (C) Validation of CD69$^+$CD154$^+$ AIM cells depicting absence from T regulatory and naive compartments (left) and inclusion of all cytokine-producing cells (right). (D) Representative flow cytometry gating of non-naive (nn) AIM CD4$^+$CD69$^+$CD154$^+$ T cells in DMSO-, M/N-, and S-stimulated memory T cells from SARS-CoV-2 naive (left, blue) and SARS-CoV-2 previously infected (right, red) participants before and 1 week after two doses of mRNA vaccine. (E and F) Summary graphs of MN- (E) and S-specific (F) nnCD4$^+$ T cells. Data in (E) and (F) are represented both longitudinally (left) and by cross-group comparisons (middle, right). *(Cont. pg 22)*

Pre-vaccination, CD4 T cells from PI donors displayed responses to both M/N and S, consistent with prior SARS-CoV-2 infection and the presence of memory cells (Figures **1D-F**), whereas responses in N donors were undetectable above individual donor background (Figures **1D-F**). Throughout the course of vaccination, responses to M/N remained negative in N donors, but endured, undiminished in PI donors at all time points, indicating that SARS-CoV-2-specific CD4 T cells primed during infection, persist at least 18 months following initial antigen exposure (Figures **1D** and **1E**). Following initial two-dose vaccination, S-reactive AIM+ CD4 T cells were significantly elevated above pre-vaccination levels in both N and PI individuals, with no significant differences in peak CD4 T cell response between groups (Figures **1D** and **1F**). Therefore COVID-19 vaccination induces numerically equivalent populations of S-specific cells in all subjects, regardless of prior SARS-CoV-2 exposure status, that persist for at least three months.

During T cell priming, the context of the initial antigen exposure directs CD4 T cells towards different helper and memory fates with distinct functional capacities. To determine how a primary infection versus vaccination or total number of antigen exposures differentially impacted functional outcomes, we directly interrogated cytokine production from SARS-CoV-2-specific CD4 T cells following stimulation with M/N or S peptide pools in N and PI individuals. As demonstrated previously, CD154 and CD69 can be used to identify activated, antigen-reactive T cells that represent the primary cytokine producers in response to stimulation (Figures **1B** and **1C**). In PI subjects, we measured a strong cytokine response to infection in M/N- (Figure **2A–2E**) and S-reactive T cells (Figures **3C–3F, 4A, and 4B**) that was dominated by the production of

---

(cont. from Fig 1): Lines connecting data points indicate paired samples from the same donor. Significance was determined by Wilcoxon matched-paired signed rank test for longitudinal analyses and multiple unpaired Mann-Whitney test for group analyses: not significant (ns), $^{*}p < 0.05$, $^{**}p < 0.01$, $^{***}p < 0.001$. Error bars represent mean and SD. Dashed lines indicate average donor background level. Pre-vaccination (Pre), 1 week post two-dose COVID-19 mRNA vaccination (1w PV2), 3 months post two-dose vaccination (3m PV2), 2 weeks post third vaccination dose (2w PV3).

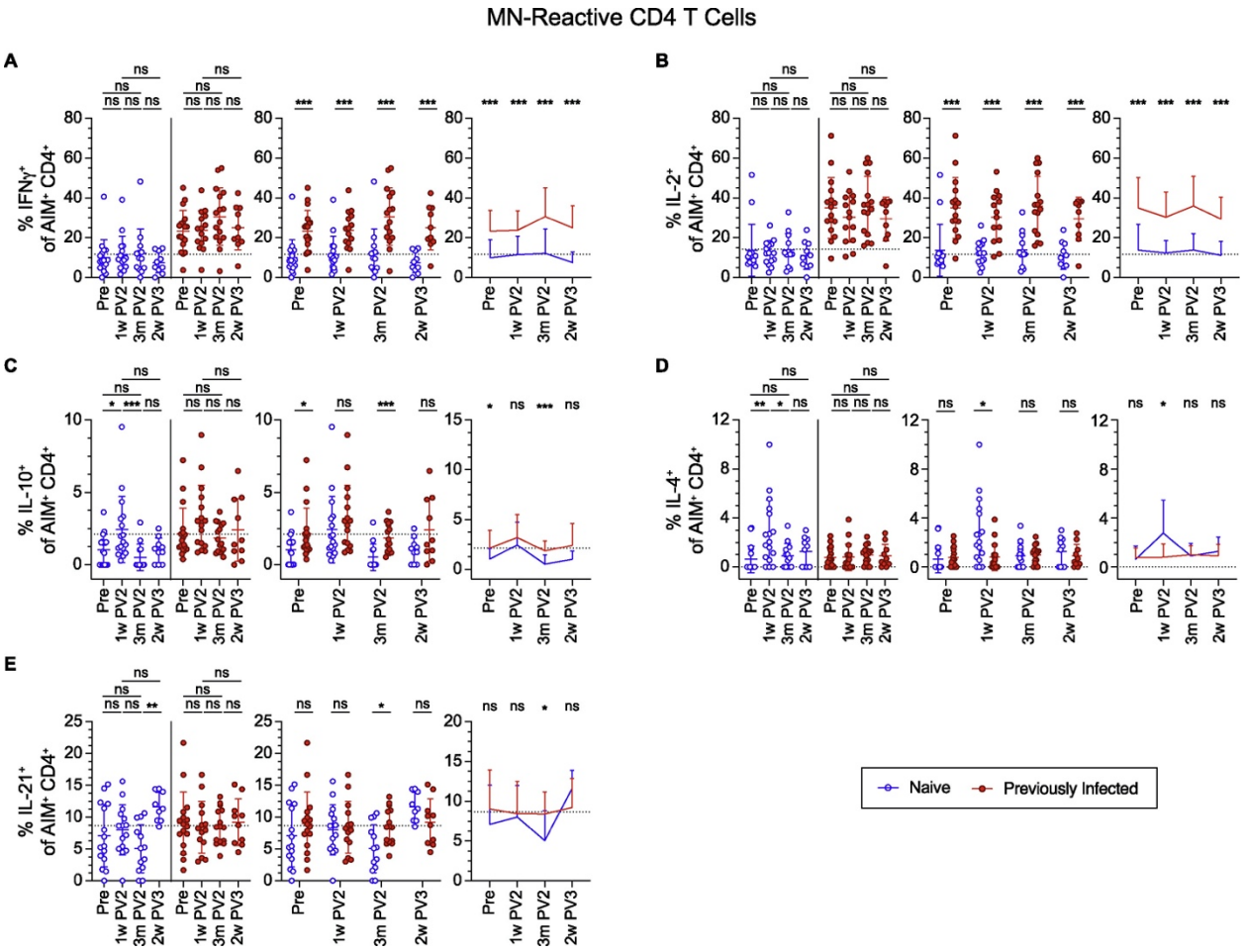

Figure 2: Cytokine production by M/N-specific AIM⁺ CD4 T cells. (A–E) Summary graphs of the indicated cytokines for M/N-specific CD4⁺CD69⁺CD154⁺ T cells (AIM⁺CD4⁺) in SARS-CoV-2 naive (blue) and previously infected (red) participants. Data are represented both longitudinally (left) and by cross-group comparisons (middle, right). Significance was determined by Wilcoxon matched-paired signed rank test for longitudinal analyses and multiple unpaired Mann-Whitney test for group analyses: not significant (ns), $^{*}p < 0.05$, $^{**}p < 0.01$, $^{***}p < 0.001$. Error bars represent mean and SD. Dashed lines indicate average donor background level. Pre-vaccination (Pre), 1 week post two-dose COVID-19 mRNA vaccination (1w PV2), 3 months post two-dose vaccination (3m PV2), 2 weeks post third vaccination dose (2w PV3).

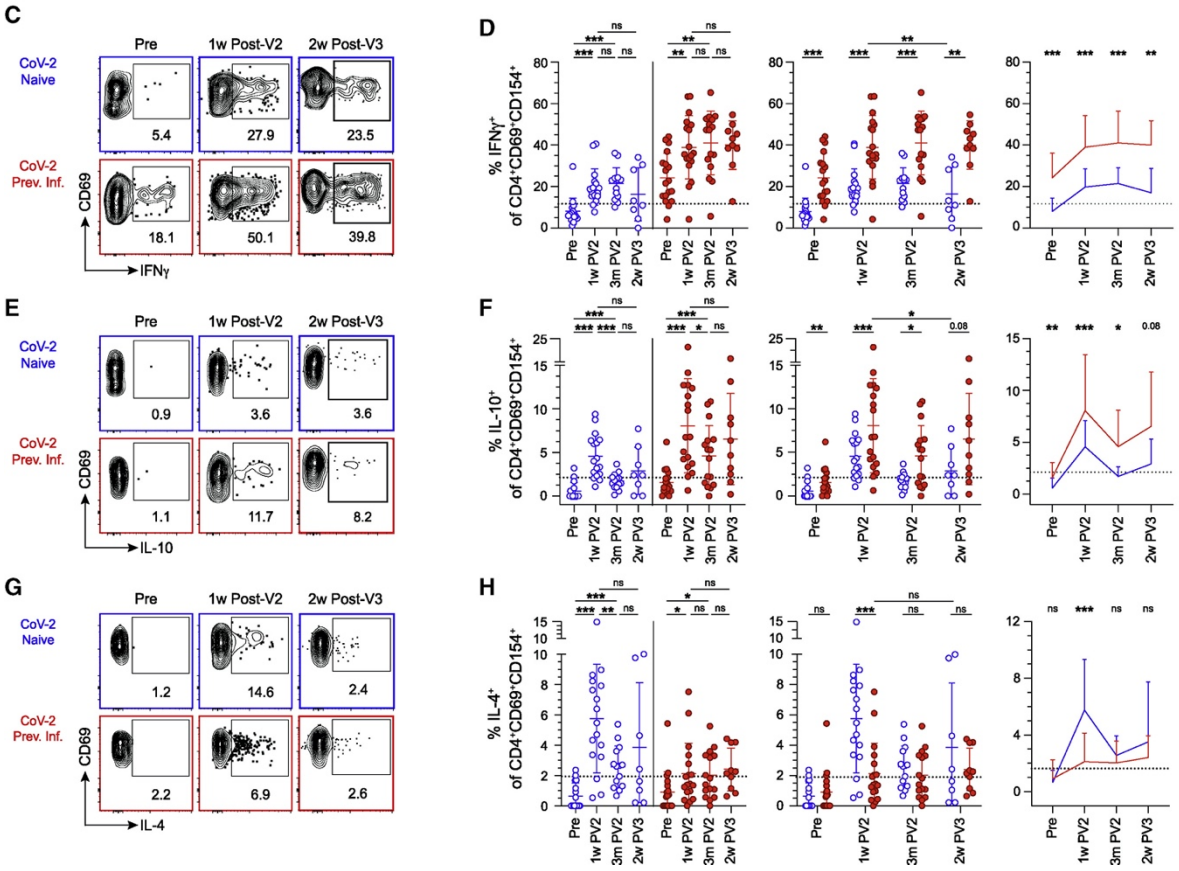

Figure 3: CD4 T cell responses to SARS-CoV-2 demonstrate qualitative effector cell differences between previously naive and previously infected individuals. Analysis of spike-reactive CD4 T cells in SARS-CoV-2 naive (blue) and previously infected (red) individuals. (C–H) Representative flow cytometry plots and summary graphs for the indicated cytokines, gated on total $CD4^+CD69^+CD154^+$ T cells. Data in (D), (F), and (H) are represented both longitudinally (left) and by cross-group comparisons (middle, right). Significance was determined by Wilcoxon matched-paired signed rank test for longitudinal analyses and multiple unpaired Mann-Whitney test for group analyses: not significant (ns), $^*p < 0.05$, $^{**}p < 0.01$, $^{***}p < 0.001$, and $^{****}p < 0.0001$. Error bars represent mean and SD. Dashed lines indicate average donor background level. Pre-vaccination (Pre), 1 week post two-dose COVID-19 mRNA vaccination (1w PV2), 3 months post two-dose vaccination (3m PV2), 2 weeks post third vaccination dose (2w PV3).

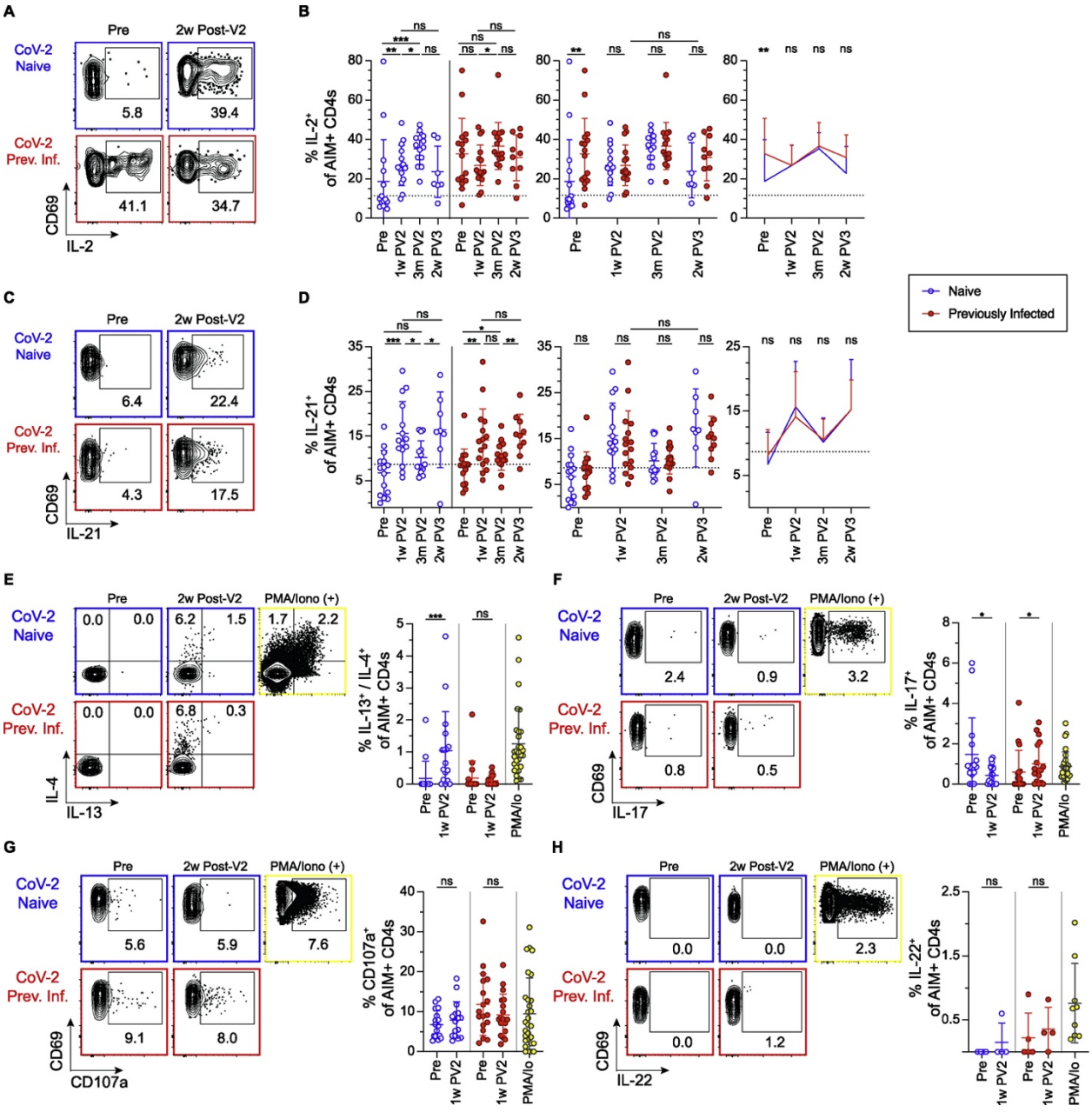

<u>Figure 4:</u> Additional cytokine production by S-specific AIM+ CD4 T cells. (A–H) Representative flow cytometry plots and summary graphs for non-naive $CD4^+CD69^+CD154^+$ T cells (AIM^+ CD4s) for the indicated cytokines. Data in (B) and (D) are represented both longitudinally (left) and by cross-group comparisons (middle, right). Validation of cytokine staining for cases of very low cytokine producers indicated in (E) through (H) are provided using phorbol 12-myristate 13-acetate (PMA) and ionomycin positive control (yellow). Significance was determined by Wilcoxon matched-paired signed rank test for longitudinal analyses and multiple unpaired *(cont. pg. 26)*

IFN-g and IL-2 but also included modest levels of IL-10. Cytokine production in response to M/N peptides in PI individuals was not enhanced by vaccination (Figure **2A–2E**). Neither N nor PI donor S-reactive T cells produced any detectable IL-4 (Figures **3G** and **3H**), IL-21, IL-13, IL-17, CD107a, or IL-22 (Figure **4C–H**) prior to vaccination. The response in N individuals to two doses of vaccination generated a functionally diverse CD4 T cell response, exhibiting strong induction of IFN-g, IL-10, IL-4 (Figure **3C–3H**), IL-2, and IL-21 (Figure **4A–4D**), whereas we observed no increased expression of IL-17A, CD107a, or IL-22 over pre-vaccination levels (Figure **4F–H**). IL-4 production, a hallmark of both Th2 and Tfh CD4 T cell responses [97], was enriched specifically at 1-week post-vaccination in N individuals (Figures **3G** and **3H**). However, few spike-reactive T cells co-produced IL-4 and IL-13 (Figure **4E**), suggesting the absence of bona fide Th2 polarization. Strikingly, PI individuals not only exhibited a strong induction of IFNg-producing S-reactive CD4 T cells following vaccination, but this response remained significantly elevated compared with the N group following both second and third vaccine doses (Figures **3C** and **3D**). PI donor CD4 T cells also produced higher levels of IL-10 after two-dose vaccination compared with N participants, which also trended higher after a third vaccine dose despite failing to reach statistical significance (Figures **3E** and **3F**). Production of IL-21, although not detected following infection, was observed at comparable levels in both N and PI individuals following two- and three-dose vaccination (Figures **4C** and **4D**).

(cont. from Fig 4):

Mann-Whitney test for group analyses: not significant (ns), $^{*}p < 0.05$, $^{**}p < 0.01$, $^{***}p < 0.001$. Error bars represent mean and SD. Dashed lines indicate average donor background level. Pre-vaccination (Pre), 1 week post two-dose COVID-19 mRNA vaccination (1w PV2), 3 months post two-dose vaccination (3m PV2), 2 weeks post third vaccination dose (2w PV3).

The S-reactive CD4 T cell compartment was further distilled into subpopulations using a dimensionality reduction analysis on pooled $CD154^{+}CD69^{+}$ cells from all participants. We applied uniform manifold approximation and projection (UMAP) followed by FlowSOM analysis and identified 15 distinct clusters of which 13 were expanded following infection or vaccination, and six included cells that produced cytokine(s) (Figure **5A–5P**). Two of these clusters, CL4 and CL13, were specifically enriched in PI donor T cells following vaccination. CL4 was defined largely by the production of IFN-g and low CD127 expression, indicative of terminally differentiated Th1 cells (Figure **5E**). CL13 was defined by co-production of IFN-g and IL-10, while also display- ing low CD127 expression, resembling FOXP3 type-1 regulatory (Tr1) cells (Figure **5N**). In contrast, increased vaccine-induced T cells producing IL-4 were specifically enriched in CL15 only in N participants. These cells additionally co-produced IL-2, IFN-g, and small amounts of IL- 21 (Figure **5P**), suggesting a Tfh-like phenotype. Collectively, this unbiased analysis of the S-reactive CD4 T cell compartment identifies the emergence of functionally distinct subsets, which differ following vaccination in PI and N participants according to prior SARS-CoV-2 infection history.

To determine how the number of antigen exposures may alter distinct cytokine production profiles seen in N and PI individuals, we compared S-reactive T cells from N individuals after three doses of vaccination (three antigen exposures) with those from PI individuals after two doses of vaccination (three antigen exposures). When cytokine production was assessed between triple-vaccinated N participants and double-vaccinated PI participants, the PI group maintained a dramatically elevated frequency of IFN-g- and IL-10-producing S-specific CD4 T cells compared with the N group (Figures **2C** and **2D**). These data indicate that T cell priming by infection or vaccination promotes distinct effector states in which functional differences persist through multiple vaccine doses.

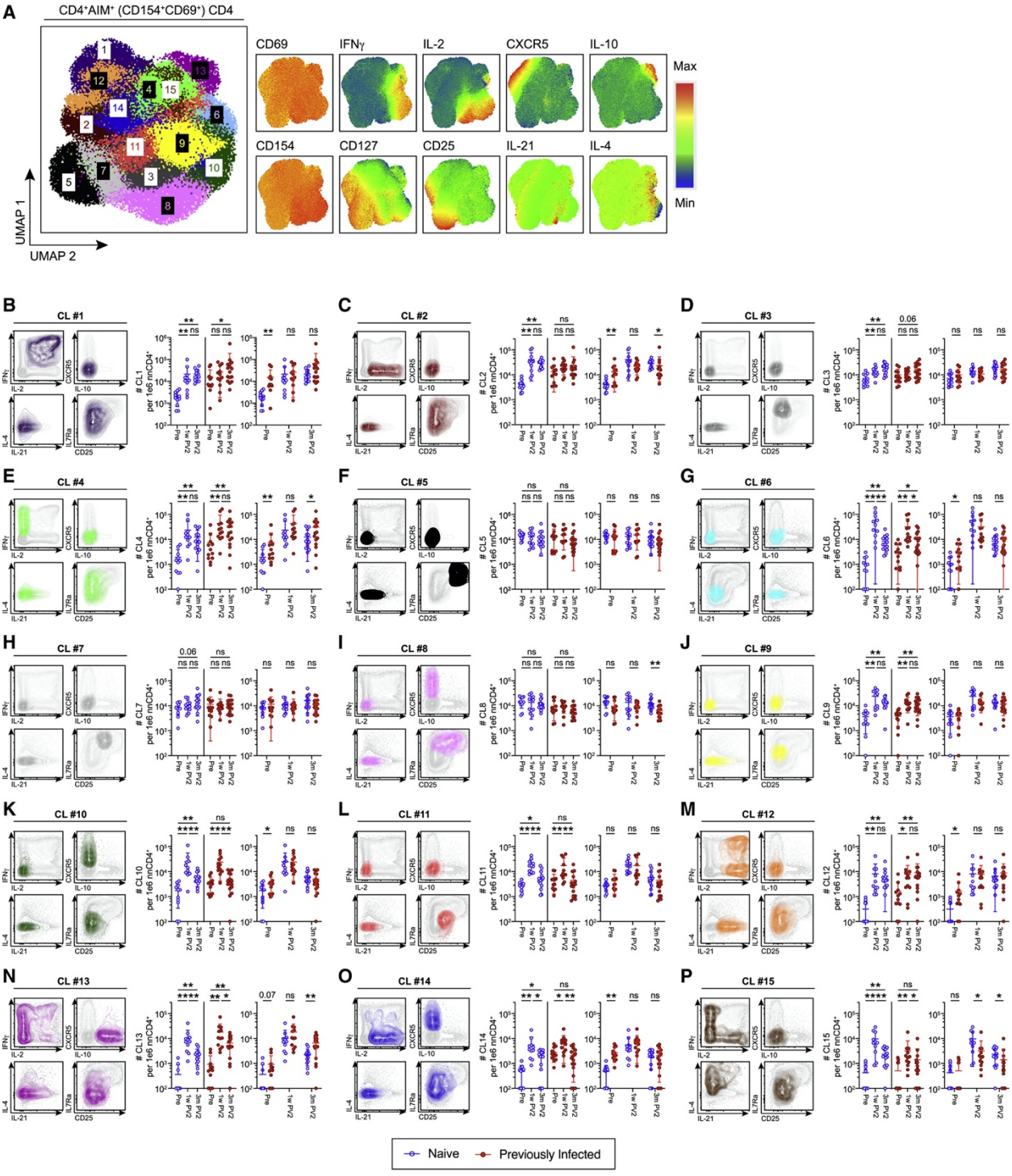

<u>Figure 5:</u> Dimensionality reduction and clustering analysis of SARS-CoV-2 S-specific CD4 AIM$^+$ T cells (A) Dimensionality reduction and phenograph-derived clustering (k = 40) overlaid for total CD4$^+$AIM$^+$(CD154$^+$CD69$^+$) T cells pooled from all participants (left). Heatmap expression of the indicated parameters over UMAP space (right). (B–P) All cells from the indicated clusters (CL) are *(cont. pg. 29)*

2.3 Discussion

Protective immunity generated in response to infection or vaccination is characterized by an expanded population of antigen-specific memory cells that rapidly expresses effector molecules upon antigen re-exposure. To prevent or control re-infection, memory cells are functionally tailored by the initial priming event; however, it is unclear how subsequent antigen exposures alter the quantity and quality of the response. The emergence of a novel coronavirus and expeditious generation of vaccines provided an unprecedented opportunity to examine the formation of a nascent antigen-specific memory pool in human volunteers and the impact of previous infection on the quantity, quality, and durability of vaccine-induced immune memory. This is particularly important, as SARS-CoV-2 infection prior to vaccination, referred to as “hybrid immunity,” provides a protective advantage over vaccination alone [83-86]. Herein, we examined the distinguishing features of hybrid immunity to SARS-CoV-2 in comparison with vaccination alone over time and with subsequent antigen exposures. We found that the spike-specific CD4 T cells induced in PI and then vaccinated individuals exhibited a unique IFN-γ and IL-10 cytokine-producing profile not recapitulated in N individuals by repeat vaccination. This represents the first immune correlate of hybrid immunity that is stably imprinted on responding cells during initial infection and could contribute to protection from symptomatic infection by providing an antiviral program.

(cont. from Figure 5): represented in corresponding color from UMAP plot in (A) overlayed on all CD4 AIM^+ T cells and showing expression of select parameters (IL-2, IFN-γ, IL-10, CXCR5, CD127, CD25, IL-4, and IL-21). Enumeration of each cluster is per 1×10^6 non-naive (nn) $CD4^+$ T cells in SARS-CoV-2 naive (blue) and SARS-CoV-2 previously infected (red) participants. Pre-vaccination (Pre), 1 week post two-dose COVID-19 mRNA vaccination (1w PV2), 3 months post two-dose vaccination (3m PV2). Significance was determined by multiple unpaired Mann-Whitney test for group analyses and by Wilcoxon matched-paired signed rank test for longitudinal analyses: not significant (ns), $^*p < 0.05$, $^{**}p < 0.01$.

Differences in route or inflammation associated with antigen exposure between N and PI individuals are likely key factors contributing to the differences in T cell phenotype and functionality associated with hybrid immunity. Pulmonary infection with SARS-CoV-2 virus and intramuscular immunization with full-length spike mRNA involve distinct inflammatory environments for immune activation to spike protein. Prolonged viral replication in pulmonary tissue has been associated with production of various inflammatory cytokines in COVID-19 patients [98-99]. Specifically, the inflammatory cytokines IL-12, IFN-α, and IFN-γ, produced by innate lymphocytes in response to viral PAMPs, directly drive T cells to upregulate the transcription factor T-bet, the master transcription factor for Th1 cells [100-101], and may induce the CD4 memory T cell IFN-γ and IL-10 signature we describe in PI individuals that is maintained through vaccination. Further, the cytokines IL-6, IL-12, or IL-27 drive the expression of IL-10 in FOXP3^{-} CD4 helper T cells through the adapter c-maf [102-104]. Functional differences, including the production of IL-10, have previously been described in SARS-CoV-2-specific CD4 T cells from individuals that experienced different levels of COVID-19 severity, raising questions about how these cytokines may be involved in immune protection [105].

Additionally, infection with SARS-CoV-2 recruits effector T cells to the lung tissue, generating tissue-resident memory cells in the human lung [106]. T cells that enter the lung tissue or interact with lung-derived innate cells in the lung-draining lymph node, may encounter a distinct inflammatory environment absent during intramuscular mRNA vaccination. Indeed, tissue-experienced CD4 Trm cells produce the highest levels of IFN-γ and IL-10 in a mouse-adapted SARS-CoV infection [30]. Therefore, it may be the case that the increase in cytokine production we see in PI participants is due to the presence of circulating S-reactive T cells, which previously received tissue-specific cues. Although primarily studied in the mouse, Trm cells have been shown to be able to re-enter the circulating memory T cell compartment from the intestine in a phenomenon termed “retrograde migration” following systemic lymphocytic choriomeningitis virus (LCMV) or vesicular stomatitis virus (VSV) infections, as well as from the

lung following influenza infection [107-109]. A similar phenomenon has also been described in humans, as skin resident CD4 Trm cells can re-enter the blood [110]. This raises the possibility that lung-transiting CoV-2-specific T cells may be captured in AIM assays of PBMCs and contribute to the increased cytokine production we observe in PI donors.

The distinct CD4 T cell cytokine signature we describe likely contributes to the increased protection observed in PI individuals with hybrid immunity. IFN-γ is produced rapidly by memory T cells *in vivo*, driving an antiviral response program, which is characterized by the upregulation of interferon-stimulated genes. Our data showing elevated frequencies of IFN-γ-producing memory CD4 T cells in PI individuals and the observed localization of CD4 Trm in the lung [106] together support a model in which early antiviral programs are bolstered rapidly by the inclusion of memory T cells locally at the site of infection. Indeed, pre-treatment of naive mice with recombinant IFN-γ completely inhibits SARS-CoV infection of the lung [30]. This study also reported that concomitant treatment with recombinant TNF-α exacerbates SARS-CoV-mediated disease in mice. IL-10 can inhibit TNF-α and other pro-inflammatory cytokines to regulate inflammatory responses to infection [35, 111-113]. Therefore, increased production of IL-10 by S-specific Th1 cells potentiated through viral infection could be a critical element of hybrid immunity that limits future symptomatic SARS-CoV-2 infection. Additional work is needed to explore this crucial role of memory T cell-derived IL-10 in secondary challenge.

The protective advantage of hybrid immunity likely stems from a combination of higher numbers of SARS-CoV-2-specific MBCs, higher neutralizing antibody titers, and the infection-imprinted IFN-γ and IL-10 cytokine profile in CD4 T cells. These features were not as highly induced in solely vaccinated individuals even with a third antigen exposure via vaccination. Future work is needed to determine how the relative timing of infection versus vaccination quantitatively and qualitatively impacts functional SARS-CoV-2 immune memory. The reduced immune response to the third vaccination in both groups as compared with the first two suggests that further homologous vaccinations are unlikely to bolster SARS-CoV-2 cellular

immune memory. Therefore, as additional viral variants evolve to further evade immune memory, future vaccination strategies should focus on expanding the pool of SARS-CoV-2-specific memory cells and increasing the titers of viral variant-neutralizing antibodies. To do this, additional vaccine doses likely need to include variant spike proteins to engage a broader repertoire of immune cells and induce further cross-reactive memory responses. We find that immunization of mice with mRNA-LNP vaccines provides incomplete benefits compared to unexposed naïve and previously infected mice. We observe that the dynamics of viral clearance mirrors the kinetics of local recruitment of NP-specific T cells to the lung mucosa and their differentiation into bonified tissue-adapted T cells.

3 Delayed mucosal localization and differentiation dynamics of the memory T cell compartment defines suboptimal protection from viral rechallenge in mRNA-LNP-vaccinated mice.

3.1 Introduction

The generation and mass implementation of pseudouridine-modified mRNA vaccines encoding the SARS-CoV-2 Spike RBD protein saved millions of lives during the COVID-19 pandemic due to its ability to generate long-lived antibody secreting plasma cells (LLPCs) and memory B and T lymphocytes able to reactivate rapidly into secondary effector cells in response to SARS-CoV-2 infection. Indeed, circulating antibodies produced by LLPCs have been shown to neutralize SARS-CoV-2 virus by binding to key viral determinants of the RBD protein, and much attention and praise was given to their role in restricting viral entry and SARS-CoV-2 infection. Unfortunately, over time, mutations in the SARS-CoV-2 spike RBD protein developed, which were driven by evolutionary pressures in population-wide immunity or isolated cases of immunosuppressed individuals receiving monoclonal antibody therapy. Mutated variants of concern (VOCs) emerged during the second and third phases of the COVID-19 pandemic, causing infection rates to dramatically increase due to the mutation of neutralizing epitopes on the SARS-CoV-2 RBD protein. Even so, infections in previously infected or vaccinated individuals displayed mild symptomology, and rates of death in immunized/infected cohorts remained significantly lower compared to unexposed individuals. This phenomenon implicated that there existed other arms of the immune system that could facilitate viral clearance and symptom recovery in the absence of neutralizing antibodies in individuals previously infected with SARS-CoV-2 or vaccinated with mRNA-LNP constructs.

T cell memory was implicated as one feature of mRNA-LNP vaccination that could facilitate viral clearance upon infection. Memory T cells retain the ability to respond to homologous

or heterologous viral antigens both through their ability to bind peptide:MHCs (pMHCs) with a broad range of receptor affinities and through their capacity to respond to intracellular proteins that may have avoided antibody-mediated immune pressure. This is important because many of the intracellular antigens are critical, highly conserved housekeeping proteins necessary for viral replication and function. For example, memory CD4 and CD8 T cells elicited by seasonal influenza A infection can be rapidly activated ex vivo in response to elements of pandemic strains of influenza, including H5N1, H3N2, and H1N1, and their presence correlates inversely with disease severity, even in the absence of neutralizing antibodies. When analyzed in more detail, T cell cross-reactivity to pandemic strains was heavily enriched for clones specific to the internal proteins nucleoprotein (NP) and M1, supporting the notion that internal proteins are more highly conserved between seasonal and pandemic strains of virus. It is currently unknown whether mRNA-LNP vaccination generates a memory T cell compartment capable of facilitating viral clearance upon a productive infection. Further, little is known concerning the dynamics of T cell localization, function, and phenotype of mRNA-LNP vaccine-generated T cell responses. Therefore, we aimed to define the mRNA-LNP vaccine-generated T cell compartment in mice, and test memory T cell-mediated clearance of respiratory viral challenge.

To determine if mRNA-LNP vaccination could generate a protective memory T cell response in the absence of neutralizing antibodies, we developed a murine system of mRNA-LNP immunization and challenge. To do this, we received pseudouridine-modified mRNA-LNP vaccine constructs which encoded the nucleoprotein from influenza A virus PR8 and X31 strains. To test the dynamics of T cell-mediated protection in the absence of neutralizing antibodies, we intranasally administered a sub-lethal challenge of X31-strain influenza virus to mRNA-LNP vaccinated mice. To further define the mRNA-LNP vaccine-generated T cell landscape, we developed MHC tetramer reagents to track the NP-specific T cell compartment in mRNA-LNP immunized mice in various anatomical compartments and across three timepoints during viral challenge.

3.2 Results

Memory T cells in a diverse range of model systems can engage in both direct and indirect antiviral effector functions in tissues to facilitate viral clearance. To interrogate the quality of LNP-mRNA vaccine generated memory T cell responses and test their ability to clear respiratory viral rechallenge, mice were immunized twice- 3 weeks apart- ipsilaterally in the quadricep muscle with 2ug of pseudouridine-modified mRNA-LNP encoding the nucleoprotein (NP) of influenza A virus (IAV) strain PR8 and X31 (Figure **6A**). We compared the dynamics of heterologous viral challenge with 1000 pfu X31 influenza virus in mRNA-vaccinated mice to both unexposed naïve mice, and to mice infected intranasally with 10 plaque-forming units (pfu) of IAV PR8 administered 40 days before X31 challenge. Viral challenge with influenza X31 specifically interrogates the ability of memory lymphocytes to clear virus, as all neutralizing antibody epitopes are disparate between PR8 and X31. Internal viral determinates such as the NP protein are conserved, allowing for activation of NP-specific memory T cells.

mRNA-LNP immunization generated both CD4 and CD8 T cell memory specific to influenza NP, visualized by MHC-tetramer staining and enrichment utilizing NP_{311} MHC-II I-$A^{(b)}$ and NP_{366} MHC-I H2-$D^{(b)}$ reagents, respectively (Figure **6B**). Upon X31 challenge, mice containing NP-specific memory T cells generated from a previous influenza infection with PR8 (IAV) displayed minor losses in weight (Figure **6C)** and were able to rapidly clear virus from the lung within 8 days (Figure **6D**), as previously described. In comparison, mice containing memory T cells generated from mRNA-LNP-vaccination lost considerable weight during the first week of challenge, resembling dynamics observed in unexposed naïve mice (Figure **6C**). Additionally, mRNA-LNP mice failed to match PR8 IAV mice in the rate of viral clearance from the lung tissue (Figure **6D**), suggesting incomplete immune protection by the memory T cell compartment following mRNA-LNP vaccination. Importantly, pulmonary viral burdens in mice with mRNA-LNP vaccine-generated memory T cells were significantly reduced compared to unexposed naïve mice

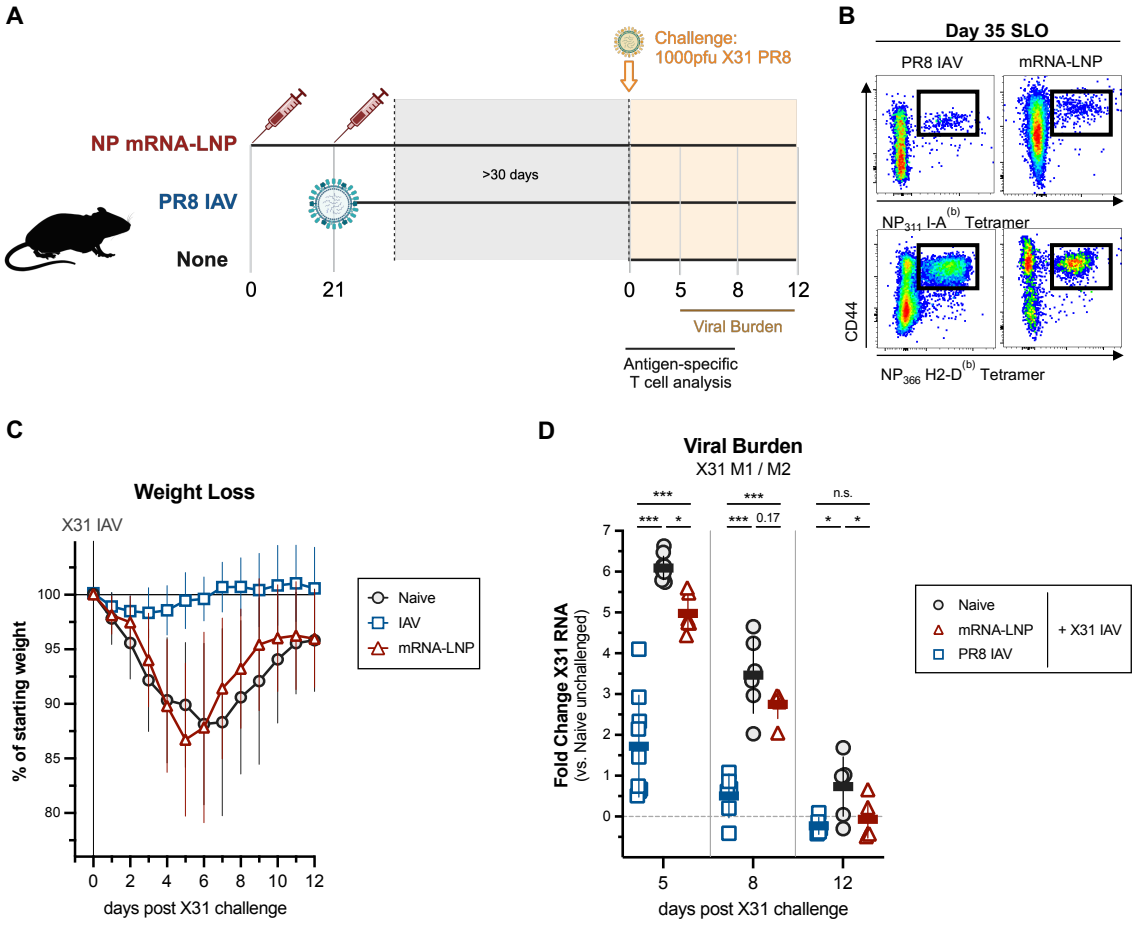

Figure 6: mRNA-LNP vaccine-generated memory T cells provide an incomplete benefit compared to naïve and previously infected mice. Mice were infected with PR8 IAV, immunized twice with 2ug NP mRNA-LNP, or unmanipulated before challenging with X31 influenza strain >30 days after last antigen exposure (A). (B) Representative MHC-II (above) and MHC-I (below) tetramer staining in lymphoid compartment of IAV-infected (left) or mRNA-LNP immunized (right) mice at day 35. (C) Kinetics of weight loss following X31 challenge (X31 IAV; grey line). Data pooled and displayed together from 4 separate experiments in equivalent numbers of male and female mice in each exposure group. (D) X31 viral M1/M2 RNA burden in lungs of X31 challenge mice depicted on days 5, 8, and 12 post-challenge. All data points normalized to log-fold change over uninfected control mice; null zero burdens. Significance was determined by multiple unpaired Mann-Whitney test for group analyses: not significant (ns), *p < 0.05, **p < 0.01, ***p < 0.001. Error bars represent mean and SD.

at days 5 and 12 post-X31 challenge, with viral burdens approaching significance at day 8 post-X31 (Figure **6D**). Therefore, the immune memory compartment generated by intramuscular mRNA-LNP vaccination provides a significant advantage over unexposed naïve mice but could benefit from aspects of immune memory engendered by previous IAV infection.

As local T cell functions in the respiratory tract have been demonstrated to provide superior protection during viral challenge [18], we were next interested in visualizing the NP-specific CD4 and CD8 T cell compartments in the lungs of challenged mice. To visualize extravascular lung-localized antigen-specific T cells we utilized our MHC tetramer binding and enrichment strategy (Figure **6B**) in combination with intravascular antibody labelling (Figures **7A** and **7G**). Using this technique, we observe NP-specific CD4 and CD8 T cells in the extravascular lung regions of IAV mice before X31 challenge (Figures **7A** and **7G**), confirming a decade of studies describing the generation of tissue-localized T cell resident memory in mucosa following infection. In stark contrast, the NP-specific CD4 and CD8 T cells enriched from lungs of mRNA-LNP mice before X31 challenge were bound by the intravascular label (Figures **7A** and **7G**), indicating their localization in blood vessels and not lung tissue. Both IAV and mRNA-LNP mice displayed comparable levels of NP-specific CD4 T cells in the circulation and lymphoid compartments (Figures **7E** and **7F**) whereas IAV mice displayed modestly increased numbers of NP-specific CD8 T cells compared to mRNA-LNP mice before X31 challenge (Figures **7K** and **7L**). Therefore, although mRNA-LNP vaccination generated a relatively comparable memory T cell compartment in the circulation and lymphoid compartment, it generated incomplete T cell memory in extravascular lung regions, suggesting the absence of a bonified lung-resident memory T cell pool.

Since mRNA-LNP mice benefited from improved viral clearance compared to unexposed naïve mice, we were interested to determine whether NP-specific T cells enter the lung following X31 challenge and how the kinetics of entry compared to the *de novo* immune response in naïve

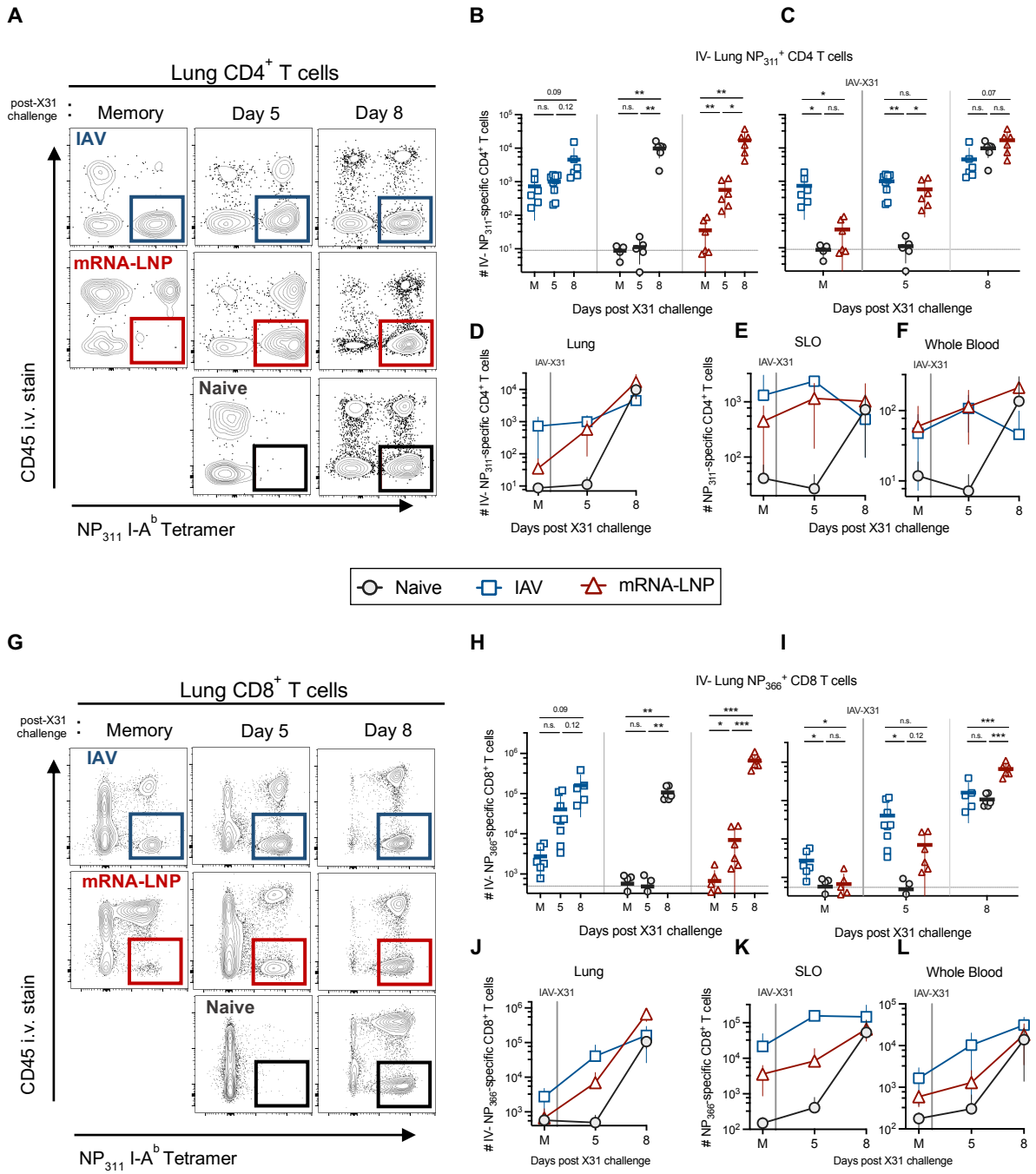

Figure 7: mRNA-LNP vaccination does not induce mucosal T cell memory but does provide expedited recruitment to lung niches. (A,G) Representative MHC-tetramer and intravascular labelling flow cytometry plots depicting extravascular NP-specific T cells following X31 challenge. (B-D; H-J) Enumeration of extravascular NP-specific T cells depicted longitudinally (left), compared between groups (right), and on an XY plot (below, left). (E-F; K-L) NP-specific T cell numbers in the lymphoid *(cont. pg. 39)*

mice. To do this, we visualized NP tetramer bound CD4 and CD8 T cells in extravascular regions of the lung at days 5 and 8 following influenza X31 challenge (Figures **7A** and **7G**) in all three groups of mice. IAV mice displayed no increase in the extravascular NP-specific CD4 T cell compartment over pre challenge numbers (Figure **7B**), suggesting that the quantity of CD4 resident memory T cells seeded by PR8 infection is sufficient to facilitate antiviral mechanisms at challenge. In unexposed naïve mice undergoing a *de novo* primary T cell response, we did not observe NP-specific CD4 T cells in the circulation, lymphoid, or lung compartments until day 8 post-X31 in line with previous data from our lab tracking the primary response to influenza infection. In contrast, we could successfully visualize extravascular NP-specific CD4 T cells in the lungs of mRNA-LNP mice by day 5 post-X31 challenge, which were further increased when analyzed at day 8 post-X31 (Figure **7A-7D**). When compared over time, although lungs of IAV mice harbor CD4 T cells in the tissues before challenge, both mRNA-LNP and unexposed naïve mice generate extravascular localized CD4 T cells by day 8 post-X31 (Figure **7A-7D**). Although not at similar numbers to IAV mice (Figure **7C**), mRNA-LNP mice display a considerable extravascular NP-specific CD4 T cell compartment at day 5, indicating an expedited recruitment of NP-specific CD4 T cells to the lungs in mRNA-LNP vaccination compared to unexposed naïve mice (Figure **7B-D**).

In contrast to the extravascular NP-specific CD4 T cell compartment, CD8 T cells displayed a dramatic numerical increase in the lungs of IAV mice post-X31 challenge, increasing by almost 100-fold over pre-challenge levels in the lungs (Figure **7H**). Similar to the CD4 T cells, mRNA-LNP mice displayed expedited recruitment of NP-specific CD8 T cells into extravascular

---

(cont. from Fig 7): and circulating compartments depicted as XY plots before and after X31 challenge. Significance was determined by multiple unpaired Mann-Whitney test for group analyses and by Wilcoxon matched-paired signed rank test for longitudinal analyses: not significant (ns), $^{*}p < 0.05$, $^{**}p < 0.01$, $^{***}p < 0.001$. Error bars represent mean and SD.

lung regions by day 5, whereas these cells were not observed until day 8 in unexposed naïve mice (Figure **7G-7J**). We believe the recruitment and expansion of extravascular NP-specific CD8 T cells in mRNA-LNP mice most likely occurs between days 5 and 8, as we observed limited numbers of these cells at day 5 post-X31 compared to IAV mice (Figure **7I**), and we detected a massive 100-fold increase in extravascular NP-specific CD8 T cell numbers between days 5 and 8 post-challenge (Figure **7H**). By day 8 post-X31 challenge all mice contained extravascular NP-specific CD8 T cells, although mRNA-LNP mice harbored significantly more of these cells at this time (Figure **7I**), a phenomenon we do not have an explanation for yet. Together, the visualization of extravascular NP-specific CD4 and CD8 T cell compartments before and early after X31 challenge indicated that mRNA-LNP vaccination does not provide resting T cell memory in the lung but does provide expedited recruitment of NP-specific CD4 and CD8 T cells to the extravascular regions of the lung by day 5 post-challenge, an occurrence not seen until day 8 in unexposed naïve mice.

We, and others, have developed a keen interest in defining the diversification of effector functions in the resident memory CD4 T cell compartment within the lungs. It has been demonstrated that there exists a T follicular-helper-like population in the extravascular regions of IAV-infected lungs which are highly important for orchestrating the tissue-immune niche by signaling to B cells, dendritic cells, and CD8 T cells [48-49]. Because of the differences in viral burden we observe between mRNA-LNP and IAV mice, but the numerically similar compartment of NP-specific CD4 T cells at days 5 and 8, we were interested to see if there were differences in phenotypic differentiation states within the tissue microenvironment early post-challenge that may contribute to reduced viral clearance. To do this, we analyzed the extravascular NP-specific CD4 T cells for the expression of CXCR6 and FR4, which are established markers we use in the lab to stratify three distinct CD4 T cell populations in the lung mucosa (Figure **8A**). Folate receptor 4 (FR4), is a marker described previously [48-49] and marks cells in iBALT displaying features of T follicular helper (T_{fh}) cells. Conversely, CXCR6 is a marker for cells which migrate away from

iBALT niches and toward the airways, which directly express the CXCR6-ligand CXCL16. Using these two markers, we can visualize FR4^{hi}CXCR6^{-} cells, FR4^{lo}CXCR6^{+} cells, and FR4^{int}CXCR6^{+} cells which we believe each occupy distinct locations and provide unique antiviral functions (Figure **8A**). As previously described, many NP-specific CD4 T cells in the lungs are FR4^{hi} at memory timepoints after PR8 infection, representing the iBALT-localized T_{fh}-like cells [48-49]. The remaining cells fall in one of the CXCR6^{+} quadrants, likely residing near or within airways (Figure **8A**). Upon X31-challenge, NP-specific CD4 T cells in IAV mice display a rapid increase in the FR4^{lo}CXCR6^{+} population which is apparent at days 5 and 8 post-challenge. The FR4^{hi}CXCR6^{-} population seen in abundance pre-challenge remained constant in all timepoints analyzed. In stark contrast to what is seen in IAV mice, the NP-specific CD4 T cells in mRNA-LNP mice are almost exclusively found in the FR4^{int}CXCR6^{+} quadrant at day 5, with little generation of cells in the FR4^{hi}CXCR6^{-} or FR4^{lo}CXCR6^{+} quadrants (Figure **8A**). We observed a similar pattern of expression on NP-specific CD4 T cells from naïve mice at day 8 post-X31 (Figure **8A**). We believe that cells recently recruited from the circulation fall into the FR4^{int}CXCR6^{+} quadrant upon entering the lung tissue. This hypothesis is supported by the kinetics of T cell entry we observe and report in **Figure 7**, in which the mRNA-LNP mice recruit cells to the lung by day 5, whereas the unexposed naïve mice require an additional 3 days to drive cells to the lung. Most interestingly, we observe that by day 8, the NP-specific CD4 T cell compartment in the mRNA-LNP mice begin to diversify and populate the FR4^{lo}CXCR6^{+} and FR4^{hi}CXCR6^{-} quadrants (Figure **8A**). By day 8, the NP-specific CD4 T cell compartment in mRNA-LNP mice contains similar frequencies of FR4^{lo}CXCR6^{+} and FR4^{hi}CXCR6^{-} cells in comparison to IAV mice (Figures **8B** and **8C**). These data suggest that between days 5 and 8, the NP-specific CD4 T cells in mRNA-LNP mice further differentiate in response to currently unknown tissue-localized factors to resemble the population of T cells in IAV mice at all timepoints during challenge.

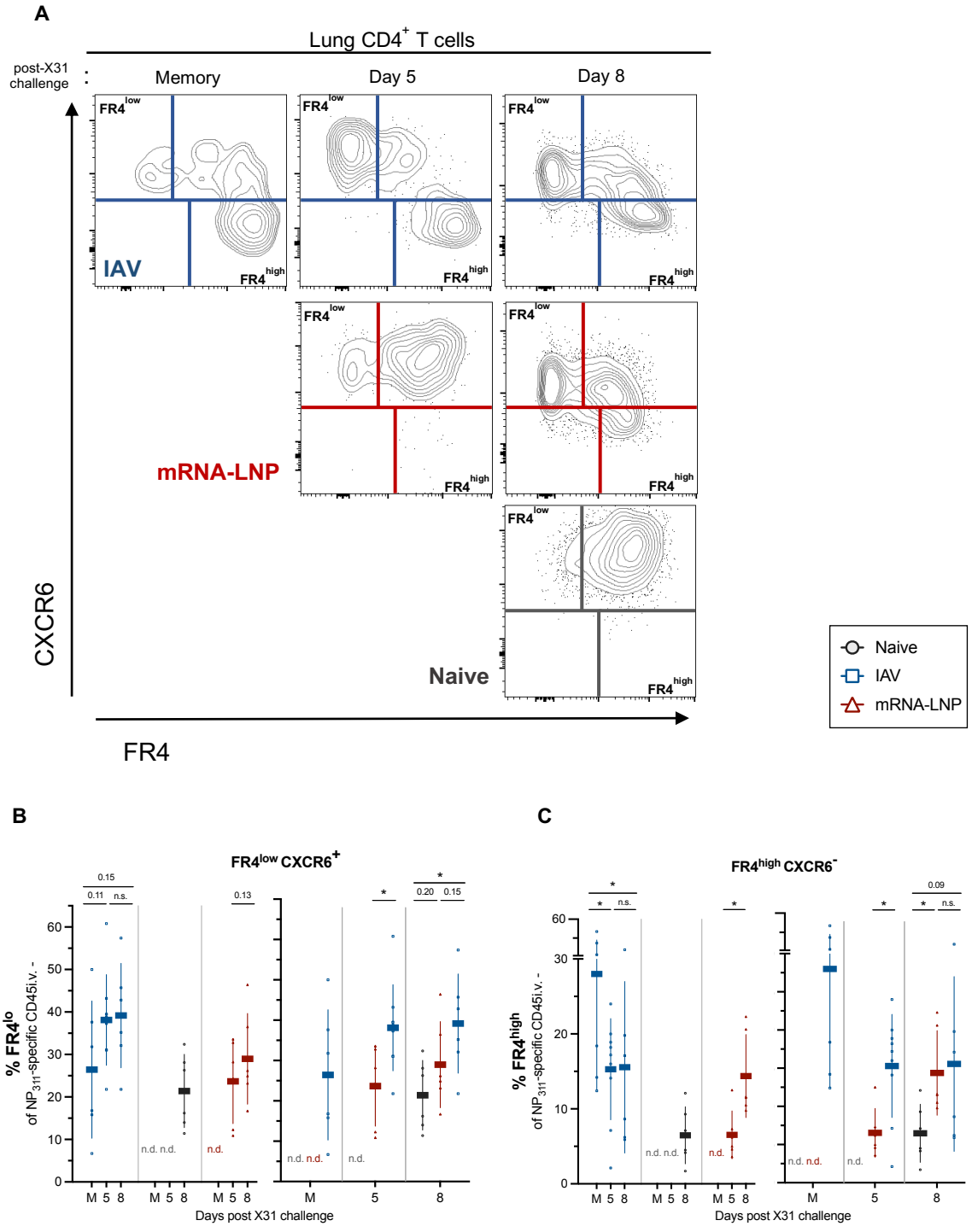

Figure 8: mRNA-LNP vaccine-generated CD4 T cells display delayed acquisition of tissue-adapted phenotypes. (A) Representative flow cytometry staining of extravascular NP-specific CD4 T cells in the lungs of mRNA-LNP (red), IAV (blue), and unexposed naïve (black) mice *(cont. pg. 42)*

In conclusion, we observe incomplete protection from viral challenge in mRNA-LNP-vaccinated mice compared to IAV mice, but improved protection compared to unexposed naïve mice. Predictive of weight loss and viral burdens, IAV mice generated memory T cells at the earliest possible timepoint, with CD4 and CD8 T cells being localized in tissues before challenge was administered. Additionally, memory CD4 T cells in IAV mice had time to perceive unique tissue factors and were engendered with a tissue-specific phenotype before challenge was administered. In contrast, T cells from mRNA-LNP mice were not observed until day 5 after challenge and did not display tissue phenotypes paralleling those which are observed in IAV mice until day 8 post-X31. Even so, T cells from mRNA-LNP mice entered the lungs and differentiated in a more expedited fashion compared to unexposed naïve mice, signifying a beneficial advantage of the generation of circulating memory T cells in comparison to the absence of a virus-specific T cell compartment. The analysis of the kinetics and phenotypes of memory T cells in the lungs was predictive of viral burden dynamics, where mRNA-LNP mice displayed intermediate phenotypes for both metrics. Together, these data suggest that intramuscular mRNA-LNP vaccination provides significant, but limited, memory T cell-facilitated protection over unexposed mice which is defined by the ability of T cells to quickly localize to mucosal sites of infection while also undergoing tissue-specific differentiation to most efficiently clear virus. Additionally, these data highlight the need to adopt aspects of infection-generated T cell memory into mRNA-LNP vaccination strategies to improve T cell vaccination regimens and ultimately protect against pandemic-strain heterologous viral infection.

(cont. from Fig. 8): at days -1 (Pre), 5, and 8 post-X31 challenge. (B, C) Frequencies of FR4hi (C) and FR4lo (B) tissue-adapted CD4 T lymphocyte populations represented longitudinally (left) and compared between groups (right); n.d. indicates too low parent (NP-specific) cell numbers to calculate frequencies accurately. Significance was determined by multiple unpaired Mann-Whitney test for group analyses and by Wilcoxon matched-paired signed rank test for longitudinal analyses: not significant (ns), $^{*}p < 0.05$, $^{**}p < 0.01$, $^{***}p < 0.001$. Error bars represent mean and SD.

3.3 Discussion

We report that mRNA-LNP vaccination generates a robust population of CD4 and CD8 memory T cells in the circulating and lymphoid compartments but failed to elicit significant cellular memory in the lung mucosa. This phenomenon has been previously described in mice, although no study had determined the capacity of the circulating memory T cell compartment to clear respiratory virus in the absence of neutralizing antibodies. This question is of particular importance because the ability to vaccinate against novel coronavirus VOCs and/or pandemic strains of influenza, which evade community levels of neutralizing antibodies, would provide a significant second arm of immunity against mortality following pandemic emergence. We observe that circulating T cell memory provides incomplete benefits, wherein IAV-primed mice perform significantly better and unexposed naïve mice significantly worse than mRNA-LNP mice at clearing virus from the infected lung mucosa.

We see that the presence of circulating memory T cells in mRNA-LNP mice expedites the recruitment of antigen-specific antiviral T cells to the lungs compared to naïve unexposed mice, which need to endure a primary immune response involving antigen trafficking and T cell priming/expansion in the lymphoid organs. This expedited recruitment is reflected in the ability of lung-localized T cells to more quickly adapt phenotypes associated with tissue-localized cells, as observed in the IAV mice. We believe the acquisition of the tissue phenotypes we describe are beneficial to efficiently clear virus from the lung mucosa and is reflected in the reduced viral burdens observed in mRNA-LNP mice compared to unexposed naïve mice. We believe IAV mice benefitted from the generation of local tissue resident memory before X31 challenge, allowing for rapid reactivation within tissues and the fastest clearance of viral burdens. Importantly, CD4 T cells from IAV mice displayed tissue-adapted phenotypes even before challenge, again signifying a benefit in having preformed mucosal immunity before viral challenge. Together, our data imply that mRNA-LNP vaccine-generated memory T cells can provide limited protective capacity in the

absence of neutralizing antibodies, but this protective benefit could be substantially improved by adapting aspects of previous infection in future vaccine regimens.

4 Concluding Remarks

Although virus-specific memory cells provide numerous benefits during a reinfection event, current vaccination strategies instead often target the development of circulating neutralizing antibodies. Studies are beginning to address the added benefits of T cells in vaccination. In a mouse model of influenza vaccination, Zens et al. [114] compared the ability of dead inactivated virus or live, attenuated influenza virus (LAIV) administered either i.m. or as an aerosol i.n. to elicit Trm cells. They found that only LAIV administered i.n. drove the development of $CD69^+$ CD8 and CD4 Trm cells that resembled canonical resident memory cells in the lung, suggesting that yearly human tri- or quadrivalent influenza vaccinations, which are administered i.m., do not drive Trm cell formation. Further, although i.m. inactivated virus drove a more potent anti-HA antibody response in the serum, only i.n. LAIV vaccination protected mice from disease after infection with a heterologous influenza strain. Studies such as these highlight the urgency for approved vaccination strategies that can drive tissue-resident memory. From studies in natural infections, we know that the generation of potent Trm cells in vivo requires numerous cellular signals occurring in both the lymphatic organs and the tissues. Although the developmental pathway driving CD4 and CD8 Trm cells are not likely identical, studies have revealed overarching tissue residency modules in lymphocytes [115], and CD4 and CD8 T cells share many similar molecular axes that can be harnessed through creative vaccination strategies to develop universal vaccines and prevent future pandemics.

Even if T cells obtain all the necessary signals in the lymphoid organs, they cannot become Trm cells without local signals in the tissue to elicit their infiltration and mediate their retention. As

mentioned above, the administration of LAIV i.n., where the antigen and inflammation were localized to the lung tissue, resulted in both CD4 and CD8 Trm cells in the tissue [114]. The necessity for local antigen was also apparent in a study that used an adenovirus vaccine platform to prolong antigen presentation in the lung for up to 80 d. As opposed to natural infection, where CD8 Trm cells seem to wane after prolonged periods of senescence [116], this platform elicited high numbers of CD8 Trm cells that were detected out to 1 year, the farthest time point analyzed [117]. In addition to antigen, T cells require help from other resident lymphocytes to facilitate their survival. In models of respiratory viral infection, CD4 Trm cells required B cells and MHCII for their long-term persistence in the lung tissue [48, 54]. Similarly, during influenza infection, CD8 Trm cells require help from the CD4-derived cytokines IFN-γ and IL-21 to localize to the airways and develop into Trm cells [49, 61]. Further, multiple studies have reported attrition of T cells in the lung [16, 116, 118] and further research into whether this attrition results in reduced protection over time or, alternatively, is the result of continuous retrograde migration of Trm cells to the lung draining LN [107-109]. Therefore, understanding how to induce parenchymal lymphatic niches through vaccination is a promising strategy to promote immune memory niches more efficiently in the tissues.

In this light, we are currently in collaboration to test a novel intranasal adjuvant strategy to recruit antigen-specific cells to the lungs during the primary vaccination schedule. This strategy, termed LION-PAMP, utilizes a RIG-I agonist to activate the lung mucosa and theoretically recruit effector T cells to the tissue to establish residence. If successful, we will hope to recapitulate the protective benefit seen in IAV mice by administering mRNA-LNP vaccines intramuscularly in combination with LION-PAMP administered intranasally.

5 Materials and Methods

Human study participants and clinical data

Participants were enrolled in one of three prospective cohort studies for longitudinal tracking of immune responses to COVID-19 vaccination in WA, USA. Previously SARS-CoV-2 infected (PI) individuals reported a positive SARS-CoV-2 PCR nasal swab or in one case a positive antibody test within 3 months of symptom onset in 2/2020- 10/2020. PI individuals reported mildly symptomatic disease not requiring hospitalization. Participants were considered SARS-CoV-2 naive (N) prior to vaccination based on no prior positive SARS-CoV-2 PCR nasal swab and no detectable SARS-CoV-2 RBD IgG by ELISA (below a threshold of mean + 3 standard deviations of historical negative plasma samples drawn prior to 2020). All participants completed surveys regarding symptom and demographic information. Blood draws were collected pre-vaccination (N: 21, PI: 23), 1 week post-vaccination 2 (N: 18, PI: 22), 3 months post-vaccination 2 (N: 15, PI: 23), 6 months post-vaccination 2 (N: 8, PI: 9) and 2 weeks post-vaccination 3 (N: 8, PI: 10).

Sample processing and plasma collection

Venous blood from study volunteers was collected in EDTA tubes and spun at 700 x g for 10 min. Plasma was collected, heat-inactivated at 56°C for 30 min and stored at -80^{o}C. Cellular fraction was resuspended in phosphate buffered saline (PBS) and PBMCs were separated from red blood cells using Sepmate PBMC Isolation Tubes (STEMCELL Technologies) according to manufacturer's instruction or cells were resuspended in HBSS, washed, overlaid with ficoll, spun at 400 x g for 30 min with no brake and PBMCs collected. Cells were washed twice in HBSS and frozen at -80^{o}C before being stored in liquid nitrogen.

Peptide mesopools

SARS-CoV-2 15-mer peptides, 1mg each (BEI Resources), were provided lyophilized and stored at -80C. Peptides were selected for reactivity against a broad range of class I and class II HLA sub-types for targeted coverage of $CD4^+$ and $CD8^+$ T cell epitopes identified previously. Before use, peptides were warmed to room temperature for 1 hour then reconstituted in DMSO to a concentration of 10 mg/mL. Individual peptides were combined in equal ratios to create Membrane/Nucleocapsid (182 ug/mL each, 55 peptides) or Spike (200ug/mL each, 49 peptides) megapools, maintaining a total concentration of 10mg/mL.

Activation induced marker assay

Approximately $20x10^6$ PBMC from SARS-CoV-2 naive or previously infected individuals were divided in two for full phenotypic or cytokine analysis. For broad surface phenotyping $10x10^6$ PBMC per sample were further divided into four 5mL polystyrene tubes and cells were pelleted at 250 x g for 5 minutes. Pellets were resuspended at $5x10^6$/mL in one of the following treatment conditions: DMSO (Sigma-Aldrich, >99.5% cell culture grade), 1ug/mL CEFX Ultra SuperStim Pool (JPT, PM-CEFX-2), or 5ug/mL SARS-CoV-2 Membrane and Nucleocapsid or Spike peptide megapools. Stimulation was performed for 18 hours in ImmunoCult-XF T cell Expansion Medium (StemCell Technologies). For intracellular cytokine assessment $2x10^6$/mL PBMC were stimulated using 6.6ug/mL SARS-CoV-2 peptide megapools, or an equivalent volume of DMSO (Sigma-Aldrich, >99.5% cell culture grade) for 12 hours in RPMI complete T cell medium containing anti-human CD40 antagonist mAb (Miltenyi, clone HB10), 5uL LAMP-1/CD107a BV510 mAb (BioLegend, clone H4A3), 2uM CaCl2, and 1.8uL Monensin (Becton Dickinson) - for the final 8 hours of culture.

Fluorescence flow cytometry

Data were acquired on a five-laser Cytek Aurora (T cell surface phenotyping and T cell intracellular cytokine analysis) or BD FACS Symphony A3 or A5 (B cell surface phenotyping). Control PBMCs or UltraComp eBeads (ThermoFisher) were used for compensation. Up to 10^7 live PBMC were acquired per sample for T cells and all enriched PBMCs were acquired for B cells. Data were analyzed using SpectroFlow (Cytek Biosciences) and FlowJo10 (Becton Dickinson) software.

High-dimensional analysis of cytometry data

AIM-positive ($CD154^+CD69^+$) cells from all data files were concatenated with keywords and subjected to Phenograph clustering algorithm using *k*=40 nearest neighbors (Levine et al., 2015) and UMAP dimensionality reduction plugins using parameters IL-2, IFN-γ, IL-10, IL-4, IL-21, CD127, CD25, and CXCR5 in FlowJo 10 (Becton Dickinson). Clusters were then enumerated per 10^6 non-naive T cells for each sample by multiplying the percentage "cluster X parameter" by percentage "AIM^+" and then by 1 million.

Mice

C57BL/6J mice were purchased from The Jackson Laboratory and maintained under specific pathogen free conditions at the University of Washington. Mice that were infected with influenza A virus Puerto Rico/8/34 H1N1 (PR8) or influenza A virus HKx31 H3N2 (X31) were housed in Animal Biosafety Level-2 conditions. Experiments were performed in accordance with the University of Washington Institutional Animal Care and Use Committee guidelines.

Viral infections and mRNA-LNP Immunizations

For influenza infections, mice were anaesthetized with ketamine/xylazine and intranasally instilled with 10 plaque forming units (pfu) of influenza A virus PR8 or 1000 pfu of influenza A virus X31 diluted in sterile PBS in a final volume of 40 µL.

For mRNA-LNP immunizations, mice were anesthetized with gaseous isoflurane and injected in the right quadriceps muscle with 2ug of pseudouridine-modified mRNA-LNPs encoding the nucleoprotein from PR8/X31 influenza virus in 50uL of sterile PBS. A second dose of 2ug mRNA-LNP was administered ipsilaterally to mice 19-22 days following the primary immunization. mRNA-LNPs were engineered, formulated, and distributed by the lab of Drew Weissman, University of Pennsylvania.

Isolation of cells from the lung

Approximately 3 minutes prior to sacrifice, mice were injected intravenously with 1 µg anti-CD45 BUV395 (BD Biosciences) to label T cells in the vasculature. Mice were then euthanized via CO2 asphyxiation and lungs were harvested into PBS with 2% fetal calf serum. The lung tissue was placed into gentleMACS C Tubes (Miltenyi Biotec) with RPMI 1640 Medium with HEPES (Gibco, #22400089) containing 70 µg/mL Liberase TM (Roche #05401127001) and 10 mM aminoguanidine (Sigma-Aldrich). The tissue was dissociated on the gentleMACS Dissociator (Miltenyi Biotec) and then incubated at 37°C for 30 minutes followed by a final dissociation step. The single cell suspensions from the lung were then filtered over 70 µm mesh and washed with Dulbecco's Modified Eagle's Medium [Corning, Inc.; Ref: 10-017-CV] with 10% fetal calf serum to inhibit liberase activity.

Viral RNA quantification

For viral RNA quantification, the right lower lung lobe was harvested from C57BL/6J mice and placed in RNAlater Stabilization Solution (Invitrogen) at -20°C. 15 mg of lung tissue was lysed

using the RNeasy Plus Mini Kit RLT buffer with b-mercaptoethanol (Qiagen) and a 5mm stainless steel bead (Qiagen) on the TissueLyser II (Qiagen) twice for 2.3 mins at 30 Hz. RNA was isolated from the lysate using the RNeasy Plus Mini Kit (Qiagen) according to manufacturer instructions. Isolated RNA was then synthesized and amplified into cDNA using the High-Capacity cDNA Reverse Transcription Kit (Thermofisher). For IAV M1/M2 measurement, this cDNA was used as a template for quantitative PCR using PrimeTime qPCR Probe Assays (Integrated DNA Technologies, Inc.) and PrimeTime Gene Expression Master Mix (Integrated DNA Technologies, Inc.) with the following primer and probe design: Probe: (6-FAM/ZEN/IBFQ) 5'- CCTCTGCTGCTTGCTCACTCGATC-3'; Forward Primer: 5'-CAGCACTACAGCTAAGGCTATG-3'; Reverse Primer: 5'-CTCATCGCTTGCACCATTTG-3'. Transcripts were normalized to Rps17 (40S ribosomal protein S17) which was quantified using PowerUP SYBR Green Master Mix (Applied Biosystems) with the primers: *Rps17* Fwd: 5'-CGCCATTATCCCCAGCAAG-3'; *Rps17* Rev: 5'- TGTCGGGATCCACCTCAATG-3'.

Cell enrichment and flow cytometry

Following acquisition of single cell suspensions, cells were stained with $NP_{311-325}$ (QVYSLIRPNENPAHK) I-A^b tetramer and $NP_{366-374}$ (ASNENMETM) H2-D^b conjugated to APC and incubated at room temperature in the dark for 1 hour. Cells were then washed and incubated with 25 μL anti-APC microbeads (Miltenyi Biotec) on ice for 30 minutes. After incubation, cells were washed and tetramer-positive cells were enriched over magnetic LS columns (Miltenyi Biotec). The enriched fraction and "flow-through" non-enriched fraction were then surfaced stained with antibody master mixes on ice for 30 minutes for downstream analysis of tetramer- specific cells and bulk lymphocyte populations. When applicable, cells were then fixed and permeabilized with eBioscience Foxp3/Transcription Factor Staining Buffer Set (Invitrogen) according to manufacturer instructions. Intracellular transcription factor staining was performed in 1X Permeabilization Buffer (Invitrogen) at room temperature for 1 hour before data

acquisition by flow cytometry. All cells were acquired on the LSR II or FACSymphony (BD) and analyzed using FlowJo 10.8.1 software (Treestar).

Statistical analysis

Statistical analysis was performed by unpaired t test, Mann-Whitney test, or Spearman's rank correlation as indicated in the figure legends using Prism 9.4.0 (GraphPad Software, San Diego, CA). Graphs show mean ± SD.

7 References

1. CasrougeA,BeaudoingE,DalleS,PannetierC,KanellopoulosJ,KourilskyP.2000.Sizeestimateof the αβ TCR repertoire of naive mouse splenocytes. *J. Immunol.* 164:5782–87
2. DavisMM,BonifaceJJ,ReichZ,LyonsD,HamplJ,etal.1998.LigandrecognitionbyαβTcellrecep- tors. *Annu. Rev. Immunol.* 16:523–44
3. Pepper M, Jenkins MK. 2011. Origins of $CD4^+$ effector and central memory T cells. *Nat. Immunol.* 12:467–71
4. SallustoF,LenigD,FörsterR,LippM,LanzavecchiaA.1999.TwosubsetsofmemoryTlymphocytes with distinct homing potentials and effector functions. *Nature* 401:708–12
5. Beura LK, Fares-Frederickson NJ, Steinert EM, Scott MC, Thompson EA, et al. 2019. $CD4^+$ resident memory T cells dominate immunosurveillance and orchestrate local recall responses. *J. Exp. Med.* 216:1214–29
6. Glennie ND, Yeramilli VA, Beiting DP, Volk SW, Weaver CT, Scott P. 2015. Skin-resident memory $CD4^+$ T cells enhance protection against *Leishmania major* infection. *J. Exp. Med.* 212:1405–14
7. Teijaro JR, Turner D, Pham Q, Wherry EJ, Lefrançois L, Farber DL. 2011. Cutting edge: Tissue-retentive lung memory CD4 T cells mediate optimal protection to respiratory virus infection. *J. Immunol.* 187:5510–14
8. ZensKD,ChenJK,FarberDL.2016.Vaccine-generatedlungtissue-residentmemoryTcellsprovide heterosubtypic protection to influenza infection. *JCI Insight* 1:85832
9. Szabo, P.A., M. Miron, and D.L. Farber. 2019. Location, location, location: Tissue resident memory T cells in mice and humans. Sci. Immunol. 4:eaas9673. https://doi.org/10.1126/sciimmunol.aas9673
10. Jameson, S.C., and D. Masopust. 2018. Understanding subset diversity in T cell memory. Immunity. 48:214–226. https://doi.org/10.1016/j.immuni .2018.02.010

11. Steinert, E.M., J.M. Schenkel, K.A. Fraser, L.K. Beura, L.S. Manlove, B.Z. Ig- ya´rtó, P.J. Southern, and D. Masopust. 2015. Quantifying memory CD8 T cells reveals regionalization of immunosurveillance. Cell. 161:737–749. https://doi.org/10.1016/j.cell.2015.03.031

12. Beura, L.K., N.J. Fares-Frederickson, E.M. Steinert, M.C. Scott, E.A. Thompson, K.A. Fraser, J.M. Schenkel, V. Vezys, and D. Masopust. 2019. $CD4^+$ resident memory T cells dominate immunosurveillance and orchestrate local recall responses. J. Exp. Med. 216:1214–1229. https://doi.org/10.1084/jem.20181365

13. Schenkel, J.M., K.A. Fraser, L.K. Beura, K.E. Pauken, V. Vezys, and D. Ma- sopust. 2014. T cell memory. Resident memory CD8 T cells trigger protective innate and adaptive immune responses. Science. 346:98–101. https://doi.org/10.1126/science.1254536

14. Iijima, N., and A. Iwasaki. 2014. T cell memory. A local macrophage che- mokine network sustains protective tissue-resident memory CD4 T cells. Science. 346:93–98. https://doi.org/10.1126/science.1257530

15. Teijaro, J.R., D. Verhoeven, C.A. Page, D. Turner, and D.L. Farber. 2010. Memory CD4 T cells direct protective responses to influenza virus in the lungs through helper-independent mechanisms. J. Virol. 84: 9217–9226. https://doi.org/10.1128/JVI.01069-10

16. Wu, T., Y. Hu, Y.T. Lee, K.R. Bouchard, A. Benechet, K. Khanna, and L.S. Cauley. 2014. Lung-resident memory CD8 T cells (TRM) are indis- pensable for optimal cross-protection against pulmonary virus infec- tion. J. Leukoc. Biol. 95:215–224. https://doi.org/10.1189/jlb.0313180

17. Slütter, B., L.L. Pewe, S.M. Kaech, and J.T. Harty. 2013. Lung airway- surveilling CXCR3(hi) memory CD8(+) T cells are critical for protection against influenza A virus. Immunity. 39:939–948. https://doi.org/10 .1016/j.immuni.2013.09.013

18. Teijaro, J.R., D. Turner, Q. Pham, E.J. Wherry, L. Lefrançois, and D.L. Farber. 2011. Cutting edge: Tissue-retentive lung memory CD4 T cells mediate optimal protection to respiratory virus infection. J. Immunol. 187: 5510–5514. https://doi.org/10.4049/jimmunol.1102243

19. Akondy, R.S., M. Fitch, S. Edupuganti, S. Yang, H.T. Kissick, K.W. Li, B.A. Youngblood, H.A. Abdelsamed, D.J. McGuire, K.W. Cohen, et al. 2017. Origin and differentiation of human memory CD8 T cells after vacci- nation. Nature. 552:362–367. https://doi.org/10.1038/nature24633

20. Araki, Y., Z. Wang, C. Zang, W.H. Wood III, D. Schones, K. Cui, T.-Y. Roh, B. Lhotsky, R.P. Wersto, W. Peng, et al. 2009. Genome-wide analysis of histone methylation reveals chromatin state-based regulation of gene transcription and function of memory CD8+ T cells. Immunity. 30: 912–925. https://doi.org/10.1016/j.immuni.2009.05.006

21. Weng, N.P., Y. Araki, and K. Subedi. 2012. The molecular basis of the memory T cell response: differential gene expression and its epigenetic regulation. Nat. Rev. Immunol. 12:306–315. https://doi.org/10.1038/nri3173

22. Lai, W., M. Yu, M.-N. Huang, F. Okoye, A.D. Keegan, and D.L. Farber. 2011. Transcriptional control of rapid recall by memory CD4 T cells. J. Immunol.187:133–140. https://doi.org/10.4049/jimmunol.1002742

23. Oja, A.E., B. Piet, C. Helbig, R. Stark, D. van der Zwan, H. Blaauwgeers, E.B.M. Remmerswaal, D. Amsen, R.E. Jonkers, P.D. Moerland, et al. 2018. Trigger happy resident memory CD4^{+} T cells inhabit the human lungs. Mucosal Immunol. 11:654–667. https://doi.org/10.1038/mi.2017.94

24. Soudja, S.M., C. Chandrabos, E. Yakob, M. Veenstra, D. Palliser, and G. Lauvau. 2014. Memory-T-cell-derived interferon-γ instructs potent innate cell activation for protective immunity. Immunity. 40:974–988. https://doi.org/10.1016/j.immuni.2014.05.005

25. Strutt, T.M., K.K. McKinstry, J.P. Dibble, C. Winchell, Y. Kuang, J.D. Curtis, G. Huston, R.W. Dutton, and S.L. Swain. 2010. Memory CD4+ T cells in- duce innate responses independently of pathogen. Nat. Med. 16: 558–564: 1p: 564. https://doi.org/10.1038/nm.2142

26. Guvenel, A., A. Jozwik, S. Ascough, S.K. Ung, S. Paterson, M. Kalyan, Z. Gardener, E. Bergstrom, S. Kar, M.S. Habibi, et al. 2020. Epitope- specific airway resident CD4+ T cell dynamics during experimental human RSV infection. J. Clin. Invest. 130:523–538. https://doi.org/10 .1172/JCI131696

27. Chapman, T.J., K. Lambert, and D.J. Topham. 2011. Rapid reactivation of ex- tralymphoid CD4 T cells during secondary infection. PLoS One. 6: e20493. https://doi.org/10.1371/journal.pone.0020493

28. Chapman, T.J., and D.J. Topham. 2010. Identification of a unique population of tissue-memory CD4+ T cells in the airways after influenza infection that is dependent on the integrin VLA-1. J. Immunol. 184:3841–3849. https://doi.org/10.4049/jimmunol.0902281

29. Moguche, A.O., S. Shafiani, C. Clemons, R.P. Larson, C. Dinh, L.E. Higdon, C.J. Cambier, J.R. Sissons, A.M. Gallegos, P.J. Fink, and K.B. Urdahl. 2015. ICOS and Bcl6-dependent pathways maintain a CD4 T cell population with memory-like properties during tuberculosis. J. Exp. Med. 212: 715–728. https://doi.org/10.1084/jem.20141518

30. Zhao, J., J. Zhao, A.K. Mangalam, R. Channappanavar, C. Fett, D.K. Meyerholz, S. Agnihothram, R.S. Baric, C.S. David, and S. Perlman. 2016. Airway memory CD4(+) T cells mediate protective immunity against emerging respiratory coronaviruses. Immunity. 44:1379–1391. https://doi.org/10 .1016/j.immuni.2016.05.006

31. Hussell, T., A. Pennycook, and P.J.M. Openshaw. 2001. Inhibition of tumor necrosis factor reduces the severity of virus-specific lung immunopathology. Eur. J. Immunol. 31(9):2566–2573. https://doi.org/10.1002/1521 -4141(200109)31:9<2566::aid-immu2566>3.0.co;2-l

32. Damjanovic, D., M. Divangahi, K. Kugathasan, C.-L. Small, A. Zganiacz, E.G. Brown, C.M. Hogaboam, J. Gauldie, and Z. Xing. 2011. Negative regu- lation of lung inflammation and immunopathology by TNF-α during acute influenza infection. Am. J. Pathol. 179:2963–2976. https://doi.org/10.1016/j.ajpath.2011.09.003

33. Sun, J., R. Madan, C.L. Karp, and T.J. Braciale. 2009. Effector T cells control lung inflammation during acute influenza virus infection by producing IL-10.Nat. Med. 15:277–284. https://doi.org/10.1038/nm.1929

34. Sun, K., L. Torres, and D.W. Metzger. 2010. A detrimental effect of interleukin-10 on protective pulmonary humoral immunity during primary influenza A virus infection. J. Virol. 84:5007–5014. https://doi .org/10.1128/JVI.02408-09

35. O'Garra, A., and P. Vieira. 2007. T(H)1 cells control themselves by producing interleukin-10. Nat. Rev. Immunol. 7:425–428. https://doi.org/10.1038/nri2097

36. McKinstry, K.K., T.M. Strutt, A. Buck, J.D. Curtis, J.P. Dibble, G. Huston, M. Tighe, H. Hamada, S. Sell, R.W. Dutton, and S.L. Swain. 2009. IL-10 deficiency unleashes an influenza-specific Th17 response and enhances survival against high-dose challenge. J. Immunol. 182:7353–7363. https://doi.org/10.4049/jimmunol.0900657

37. Strutt, T.M., K.K. McKinstry, Y. Kuang, L.M. Bradley, and S.L. Swain. 2012. Memory CD4+ T-cell-mediated protection depends on secondary effectors that are distinct from and superior to primary effectors. Proc. Natl. Acad. Sci. USA. 109:E2551–E2560. https://doi.org/10.1073/pnas.1205894109

38. Brown, D.M., S. Lee, M.L. Garcia-Hernandez, and S.L. Swain. 2012. Multi- functional CD4 cells expressing gamma interferon and perforin mediate protection against lethal influenza virus infection. J. Virol. 86:6792–6803. https://doi.org/10.1128/JVI.07172-11

39. Marshall, N.B., A.M. Vong, P. Devarajan, M.D. Brauner, Y. Kuang, R. Nayar, E.A. Schutten, C.H. Castonguay, L.J. Berg, S.L. Nutt, and S.L. Swain. 2017. NKG2C/E marks the unique cytotoxic CD4 T cell subset, ThCTL, generated by influenza infection. J. Immunol. 198:1142–1155. https://doi .org/10.4049/jimmunol.1601297

40. Qui, H.Z., A.T. Hagymasi, S. Bandyopadhyay, M.C. St Rose, R. Ramanar- asimhaiah, A. Me´noret, R.S. Mittler, S.M. Gordon, S.L. Reiner, A.T. Vella, and A.J. Adler. 2011. CD134 plus CD137 dual costimulation induces Eomesodermin in CD4 T cells to program cytotoxic Th1 differentiation. J. Immunol. 187:3555–3564. https://doi.org/10.4049/jimmunol.1101244

41. Hua, L., S. Yao, D. Pham, L. Jiang, J. Wright, D. Sawant, A.L. Dent, T.J. Braciale, M.H. Kaplan, and J. Sun. 2013. Cytokine-dependent induction of CD4+ T cells with cytotoxic potential during influenza virus infection. J. Virol. 87:11884–11893. https://doi.org/10.1128/JVI.01461-13

42. Ioannidis, I., F. Ye, B. McNally, M. Willette, and E. Flaño. 2013. Toll-like re- ceptor expression and induction of type I and type III interferons in primary airway epithelial cells. J. Virol. 87:3261–3270. https://doi.org/10 .1128/JVI.01956-12

43. Mucida, D., M.M. Husain, S. Muroi, F. van Wijk, R. Shinnakasu, Y. Naoe, B.S. Reis, Y. Huang, F. Lambolez, M. Docherty, et al. 2013. Transcriptional reprogramming of mature CD4^{+} helper T cells generates distinct MHC class II-restricted cytotoxic T lymphocytes. Nat. Immunol. 14:281–289. https://doi.org/10.1038/ni.2523

44. He, X., X. He, V.P. Dave, Y. Zhang, X. Hua, E. Nicolas, W. Xu, B.A. Roe, and D.J. Kappes. 2005. The zinc finger transcription factor Th-POK regulates CD4 versus CD8 T-cell lineage commitment. Nature. 433:826–833. https://doi.org/10.1038/nature03338

45. Wang, L., K.F. Wildt, E. Castro, Y. Xiong, L. Feigenbaum, L. Tessarollo, and R. Bosselut. 2008. The zinc finger transcription factor Zbtb7b represses CD8 lineage gene expression in peripheral CD4+ T cells. Immunity. 29: 876–887. https://doi.org/10.1016/j.immuni.2008.09.019

46. Turner, D.L., K.L. Bickham, J.J. Thome, C.Y. Kim, F. D'Ovidio, E.J. Wherry, and D.L. Farber. 2014. Lung niches for the generation and maintenance of tissue-resident memory T cells. Mucosal Immunol. 7:501–510. https://doi .org/10.1038/mi.2013.67

47. Ciucci, T., M.S. Vacchio, Y. Gao, F. Tomassoni Ardori, J. Candia, M. Mehta, Y. Zhao, B. Tran, M. Pepper, L. Tessarollo, et al. 2019. The emergence and functional fitness of memory $CD4^+$ T cells require the transcription factor Thpok. Im- munity. 50:91–105.e4. https://doi.org/10.1016/j.immuni.2018.12.019

48. Swarnalekha, N., D. Schreiner, L.C. Litzler, S. Iftikhar, D. Kirchmeier, M. Künzli, Y.M. Son, J. Sun, E.A. Moreira, and C.G. King. 2021. T resident helper cells promote humoral responses in the lung. Sci. Immunol. 6: eabb6808. https://doi.org/10.1126/sciimmunol.abb6808

49. Son, Y.M., I.S. Cheon, Y. Wu, C. Li, Z. Wang, X. Gao, Y. Chen, Y. Takahashi, Y.-X. Fu, A.L. Dent, et al. 2021. Tissue-resident $CD4^+$ T helper cells assist the development of protective respiratory B and $CD8^+$ T cell memory responses. Sci. Immunol. 6:eabb6852. https://doi.org/10.1126/sciimmunol .abb6852

50. Moyron-Quiroz, J.E., J. Rangel-Moreno, K. Kusser, L. Hartson, F. Sprague, S. Goodrich, D.L. Woodland, F.E. Lund, and T.D. Randall. 2004. Role of inducible bronchus associated lymphoid tissue (iBALT) in respiratory immunity. Nat. Med. 10:927–934. https://doi.org/10.1038/nm1091

51. Kim, D.-Y., A. Sato, S. Fukuyama, H. Sagara, T. Nagatake, I.G. Kong, K. Goda, T. Nochi, J. Kunisawa, S. Sato, et al. 2011. The airway antigen sampling system: respiratory M cells as an alternative gateway for inhaled antigens. J. Immunol. 186:4253–4262. https://doi.org/10.4049/jimmunol.0903794

52. Rangel-Moreno, J., D.M. Carragher, M. de la Luz Garcia-Hernandez, J.Y. Hwang, K. Kusser, L. Hartson, J.K. Kolls, S.A. Khader, and T.D. Randall. 2011. The development of inducible bronchus-associated lymphoid tis- sue depends on IL-17. Nat. Immunol. 12:639–646. https://doi.org/10 .1038/ni.2053

53. Denton, A.E., S. Innocentin, E.J. Carr, B.M. Bradford, F. Lafouresse, N.A. Mabbott, U. Mo¨rbe, B. Ludewig, J.R. Groom, K.L. Good-Jacobson, and M.A. Linterman. 2019. Type I interferon induces CXCL13 to support ectopic germinal center formation. J. Exp. Med. 216:621–637. https://doi.org/10.1084/jem.20181216

54. Hondowicz, B.D., K.S. Kim, M.J. Ruterbusch, G.J. Keitany, and M. Pepper. 2018. IL-2 is required for the generation of viral-specific CD4+ Th1 tissue-resident memory cells and B cells are essential for maintenance in the lung. Eur. J. Immunol. 48:80–86. https://doi.org/10.1002/eji.201746928

55. Shinoda, K., K. Hirahara, T. Iinuma, T. Ichikawa, A.S. Suzuki, K. Sugaya, D.J. Tumes, H. Yamamoto, T. Hara, S. Tani-Ichi, et al. 2016. Thy1+IL-7+ lymphatic endothelial cells in iBALT provide a survival niche for memory T-helper cells in allergic airway inflammation. Proc. Natl. Acad. Sci. USA. 113:E2842–E2851. https://doi.org/10.1073/pnas.1512600113

56. Allie, S.R., J.E. Bradley, U. Mudunuru, M.D. Schultz, B.A. Graf, F.E. Lund, and T.D. Randall. 2019. The establishment of resident memory B cells in the lung requires local antigen encounter. Nat. Immunol. 20:97–108. https:// doi.org/10.1038/s41590-018-0260-6

57. Adachi, Y., T. Onodera, Y. Yamada, R. Daio, M. Tsuiji, T. Inoue, K. Kobayashi, T. Kurosaki, M. Ato, and Y. Takahashi. 2015. Distinct germinal center selection at local sites shapes memory B cell response to viral escape. J. Exp. Med. 212:1709–1723. https://doi.org/10.1084/jem.20142284

58. Onodera, T., Y. Takahashi, Y. Yokoi, M. Ato, Y. Kodama, S. Hachimura, T. Kurosaki, and K. Kobayashi. 2012. Memory B cells in the lung partici- pate in protective humoral immune responses to pulmonary influenza virus reinfection. Proc. Natl. Acad. Sci. USA. 109:2485–2490. https://doi .org/10.1073/pnas.1115369109

59. Rao, D.A., M.F. Gurish, J.L. Marshall, K. Slowikowski, C.Y. Fonseka, Y. Liu, L.T. Donlin, L.A. Henderson, K. Wei, F. Mizoguchi, et al. 2017. Patho- logically expanded peripheral T helper cell subset drives B cells in rheumatoid arthritis. Nature. 542:110–114. https://doi.org/10.1038/ nature20810

60. Nakanishi, Y., B. Lu, C. Gerard, and A. Iwasaki. 2009. CD8(+) T lymphocyte mobilization to virus-infected tissue requires CD4(+) T-cell help. Nature. 462:510–513. https://doi.org/10.1038/nature08511

61. Laidlaw, B.J., N. Zhang, H.D. Marshall, M.M. Staron, T. Guan, Y. Hu, L.S. Cauley, J. Craft, and S.M. Kaech. 2014. CD4+ T cell help guides formation of CD103+ lung-resident memory CD8+ T cells during influenza viral infection. Im- munity. 41:633–645. https://doi.org/10.1016/j.immuni.2014.09.007

62. Laidlaw, B.J., J.E. Craft, and S.M. Kaech. 2016. The multifaceted role of CD4(+) T cells in CD8(+) T cell memory. Nat. Rev. Immunol. 16:102–111. https://doi.org/10.1038/nri.2015.10

63. Wakim, L.M., J. Waithman, N. van Rooijen, W.R. Heath, and F.R. Carbone. 2008. Dendritic cell-induced memory T cell activation in nonlymphoid tissues. Science. 319:198–202. https://doi.org/10.1126/science.1151869

64. Belz, G.T., D. Wodarz, G. Diaz, M.A. Nowak, and P.C. Doherty. 2002. Com- promised influenza virus-specific CD8(+)-T-cell memory in CD4(+)- T-cell deficient mice. J. Virol. 76:12388–12393. https://doi.org/10.1128/ JVI.76.23.12388-12393.2002

65. Rangel-Moreno, J., D.M. Carragher, M. de la Luz Garcia-Hernandez, J.Y. Hwang, K. Kusser, L. Hartson, J.K. Kolls, S.A. Khader, and T.D. Randall. 2011. The development of inducible bronchus-associated lymphoid tis- sue depends on IL-17. Nat. Immunol. 12:639–646. https://doi.org/10 .1038/ni.2053

66. Vu Van, D., K.C. Beier, L.-J. Pietzke, M.S. Al Baz, R.K. Feist, S. Gurka, E. Hamelmann, R.A. Kroczek, and A. Hutloff. 2016. Local T/B cooperation in inflamed tissues is supported by T follicular helper-like cells. Nat. Commun. 7:10875. https://doi.org/10.1038/ncomms10875

67. Monto, A.S., and K. Fukuda. 2020. Lessons From Influenza Pandemics of the Last 100 Years. Clin. Infect. Dis. 70:951–957. https://doi.org/10.1093/cid/ciz803

68. World Health Organization. 2021a. WHO Coronavirus Disease (COVID-19) Dashboard. https://covid19.who.int (accessed March 2, 2021).

69. Lam, J.H., and N. Baumgarth. 2019. The multifaceted B cell response to in- fluenza virus. J. Immunol. 202:351–359. https://doi.org/10.4049/jimmunol.1801208

70. Horimoto, T., and Y. Kawaoka. 2005. Influenza: lessons from past pandemics, warnings from current incidents. Nat. Rev. Microbiol. 3:591–600. https://doi.org/10.1038/nrmicro1208

71. Gostic, K.M., M. Ambrose, M. Worobey, and J.O. Lloyd-Smith. 2016. Potent protection against H5N1 and H7N9 influenza via childhood hemagglutinin imprinting. Science. 354:722–726. https://doi.org/10.1126/science.aag1322

72. World Health Organization. 2021b. Seasonal Influenza Fact Sheet. https:// www.who.int/news-room/fact-sheets/detail/influenza-(seasonal) (accessed February 18, 2021)

73. Wong, R., J.A. Belk, J. Govero, J.L. Uhrlaub, D. Reinartz, H. Zhao, J.M. Errico, L. D'Souza, T.J. Ripperger, J. Nikolich-Zugich, et al. 2020. Affinity-restricted memory B cells dominate recall responses to heterologous flaviviruses. Immunity. 53:1078–1094.e7. https://doi.org/10.1016/j.immuni.2020.09.001

74. Pape, K.A., J.J. Taylor, R.W. Maul, P.J. Gearhart, and M.K. Jenkins. 2011. Different B cell populations mediate early and late memory during an endogenous immune response. Science. 331:1203–1207. https://doi.org/ 10.1126/science.1201730

75. Shlomchik, M.J. 2018. Do memory B cells form secondary germinal centers? Yes and no. Cold Spring Harb. Perspect. Biol. 10:a029405. https://doi.org/10.1101/cshperspect.a029405

76. Dogan, I., B. Bertocci, V. Vilmont, F. Delbos, J. Me´gret, S. Storck, C.-A. Reynaud, and J.-C. Weill. 2009. Multiple layers of B cell memory with different effector functions. Nat. Immunol. 10:1292–1299. https://doi.org/10.1038/ni.1814

77. Chen, L., D. Zanker, K. Xiao, C. Wu, Q. Zou, and W. Chen. 2014. Im- munodominant CD4+ T-cell responses to influenza A virus in healthy individuals focus on matrix 1 and nucleoprotein. J. Virol. 88:11760–11773. https://doi.org/10.1128/JVI.01631-14

78. Richards, K.A., D. Topham, F.A. Chaves, and A.J. Sant. 2010. Cutting edge: CD4 T cells generated from encounter with seasonal influenza viruses and vaccines have broad protein specificity and can directly recog- nize naturally generated epitopes derived from the live pandemic H1N1 virus. J. Immunol. 185:4998–5002. https://doi.org/10.4049/jimmunol .1001395

79. Sridhar, S., S. Begom, A. Bermingham, K. Hoschler, W. Adamson, W. Carman, T. Bean, W. Barclay, J.J. Deeks, and A. Lalvani. 2013. Cellular immune correlates of protection against symptomatic pandemic influenza. Nat. Med. 19:1305–1312. https://doi.org/10.1038/nm.3350

80. Wilkinson, T.M., C.K.F. Li, C.S.C. Chui, A.K.Y. Huang, M. Perkins, J.C. Lieb- ner, R. Lambkin-Williams, A. Gilbert, J. Oxford, B. Nicholas, et al. 2012. Preexisting influenza-specific CD4+ T cells correlate with disease pro- tection against influenza challenge in humans. Nat. Med. 18:274–280. https://doi.org/10.1038/nm.2612

81. Lee, L.Y.-H., L.A. Ha, C. Simmons, M.D. de Jong, N.V.V. Chau, R. Schumacher, Y.C. Peng, A.J. McMichael, J.J. Farrar, G.L. Smith, et al. 2008. Memory T cells established by seasonal human influenza A infection cross-react with avian influenza A (H5N1) in healthy individuals. J. Clin. Invest. 118: 3478–3490. https://doi.org/10.1172/JCI32460

82. Sant, A.J., A.T. DiPiazza, J.L. Nayak, A. Rattan, and K.A. Richards. 2018. CD4 T cells in protection from influenza virus: Viral antigen specificity and functional potential. Immunol. Rev. 284:91–105. https://doi.org/10.1111/ imr.12662

83. Abu-Raddad, L.J., Chemaitelly, H., Ayoub, H.H., Yassine, H.M., Benslimane, F.M., Khatib, H.A.A., Tang, P., Hasan, M.R., Coyle, P., Kanaani, Z.A., et al. (2021). Protection afforded by the BNT162b2 and mRNA-1273 COVID-19 vac- cines in fully vaccinated cohorts with and without prior infection. Preprint at medRxiv. 2021.07.25.21261093.

84. Crotty, S. (2021). Hybrid immunity. Science *372*, 1392–1393.

85. Gazit, S., Shlezinger, R., Perez, G., Lotan, R., Peretz, A., Ben-Tov, A., Cohen, D., Muhsen, K., Chodick, G., and Patalon, T. (2021). Comparing SARS-CoV-2 natural immunity to vaccine-induced immunity: reinfections versus break- through infections. Preprint at Medrxiv. 2021.08.24.21262415.

86. Goldberg, Y., Mandel, M., Bar-On, Y.M., Bodenheimer, O., Freedman, L., Ash, N., Alroy-Preis, S., Huppert, A., and Milo, R. (2021). Protection and waning of natural and hybrid COVID-19 immunity. Preprint at medRxiv. 2021.12.04.21267114.

87. Reynolds, C.J., Pade, C., Gibbons, J.M., Butler, D.K., Otter, A.D., Menacho, K., Fontana, M., Smit, A., Sackville-West, J.E., Cutino-Moguel, T., et al. (2021). Prior SARS-CoV-2 infection rescues B and T cell responses to variants after first vaccine dose. Science *372*, 1418–1423.

88. Cho, A., Muecksch, F., Schaefer-Babajew, D., Wang, Z., Finkin, S., Gaebler, C., Ramos, V., Cipolla, M., Mendoza, P., Agudelo, M., et al. (2021). Anti- SARS-CoV-2 receptor-binding domain antibody evolution after mRNA vacci- nation. Nature *600*, 517–522.

89. Schmidt, F., Weisblum, Y., Rutkowska, M., Poston, D., DaSilva, J., Zhang, F., Bednarski, E., Cho, A., Schaefer-Babajew, D.J., Gaebler, C., et al. (2021b). High genetic barrier to SARS-CoV-2 polyclonal neutralizing antibody escape. Nature *600*, 512–516.

90. Stamatatos, L., Czartoski, J., Wan, Y.-H., Homad, L.J., Rubin, V., Glantz, H., Neradilek, M., Seydoux, E., Jennewein, M.F., Maccamy, A.J., et al. (2021). mRNA vaccination boosts cross-variant neutralizing antibodies elicited by SARS-CoV-2 infection. Science *372*, eabg9175.

91. Wang, Z., Muecksch, F., Schaefer-Babajew, D., Finkin, S., Viant, C., Gaebler, C., Hoffmann, H.-H., Barnes, C.O., Cipolla, M., Ramos, V., et al. (2021). Naturally enhanced neutralizing breadth against SARS-CoV-2 one year after infec- tion. Nature *595*, 426–431.

92. Corbett, K.S., Nason, M.C., Flach, B., Gagne, M., O'Connell, S., Johnston, T.S., Shah, S.N., Edara, V.V., Floyd, K., Lai, L., et al. (2021). Immune correlates of protection by mRNA-1273 vaccine against SARS-CoV-2 in nonhuman pri- mates. Science *373*, eabj0299.

93. Feng, S., Phillips, D.J., White, T., Sayal, H., Aley, P.K., Bibi, S., Dold, C., Fus- kova, M., Gilbert, S.C., Hirsch, I., et al. (2021). Correlates of protection against symptomatic and asymptomatic SARS-CoV-2 infection. Nat. Med. *27*, 2032–2040.

94. Gilbert, P.B., Montefiori, D.C., McDermott, A.B., Fong, Y., Benkeser, D., Deng, W., Zhou, H., Houchens, C.R., Martins, K., Jayashankar, L., et al. (2022). Immune correlates analysis of the mRNA-1273 COVID-19 vaccine efficacy clinical trial. Science *375*, 43–50.

95. Khoury, D.S., Cromer, D., Reynaldi, A., Schlub, T.E., Wheatley, A.K., Juno, J.A., Subbarao, K., Kent, S.J., Triccas, J.A., and Davenport, M.P. (2021). Neutralizing antibody levels are highly predictive of immune protection from symptomatic SARS-CoV-2 infection. Nat. Med. *27*, 1205–1211.

96. Tarke, A., Sidney, J., Kidd, C.K., Dan, J.M., Ramirez, S.I., Yu, E.D., Mateus, J., da Silva Antunes, R.da S., Moore, E., Rubiro, P., et al. (2021). Comprehensiveanalysis of T cell immunodominance and immunoprevalence of SARS-CoV-2 epitopes in COVID-19 cases. Cell Rep. Med. *2*, 100204.

97. Ruterbusch, M., Pruner, K.B., Shehata, L., and Pepper, M. (2020). *In vivo* CD4+ T cell differentiation and function: revisiting the Th1/Th2 paradigm. Annu. Rev. Immunol. *38*, 705–725.

98. Galani, I.-E., Rovina, N., Lampropoulou, V., Triantafyllia, V., Manioudaki, M., Pavlos, E., Koukaki, E., Fragkou, P.C., Panou, V., Rapti, V., et al. (2021). Untuned antiviral immunity in COVID-19 revealed by temporal type I/III interferon patterns and flu comparison. Nat. Immunol. *22*, 32–40.

99. Lucas, C., Wong, P., Klein, J., Castro, T.B.R., Silva, J., Sundaram, M., Elling- son, M.K., Mao, T., Oh, J.E., Israelow, B., et al. (2020). Longitudinal analysesreveal immunological misfiring in severe COVID-19. Nature *584*, 463–469.

100. Brinkmann, V., Geiger, T., Alkan, S., and Heusser, C.H. (1993). Interferon alpha increases the frequency of interferon gamma-producing human CD4+ T cells. J. Exp. Med. *178*, 1655–1663.

101. Lazarevic, V., Glimcher, L.H., and Lord, G.M. (2013). T-bet: a bridge between innate and adaptive immunity. Nat. Rev. Immunol. *13*, 777–789.

102. Gabrysova´, L., Alvarez-Martinez, M., Luisier, R., Cox, L.S., Sodenkamp, J., Hosking, C., Pe´rez-Mazliah, D., Whicher, C., Kannan, Y., Potempa, K., et al. (2018). c-Maf controls immune responses by regulating disease-specific gene networks and repressing IL-2 in CD4+ T cells. Nat. Immunol. *19*, 497507.

103. Pot, C., Jin, H., Awasthi, A., Liu, S.M., Lai, C.-Y., Madan, R., Sharpe, A.H., Karp, C.L., Miaw, S.-C., Ho, I.-C., and Kuchroo, V.K. (2009). Cutting edge: il- 27 induces the transcription factor c-Maf, cytokine IL-21, and the Costimula- tory receptor ICOS that coordinately act together to promote differentiation of IL-10-producing Tr1 cells. J. Immunol. *183*, 797–801.

104. Yang, Y., Ochando, J., Yopp, A., Bromberg, J.S., and Ding, Y. (2005). IL-6 plays a unique role in initiating c-Maf expression during early stage of CD4 T cell activation. J. Immunol. *174*, 2720–2729.

105. Le Bert, N., Clapham, H.E., Tan, A.T., Chia, W.N., Tham, C.Y.L., Lim, J.M., Ku- nasegaran, K., Tan, L.W.L., Dutertre, C.-A., Shankar, N., et al. (2021). Highly functional virus-specific cellular immune response in asymptomatic SARS- CoV-2 infection. J. Exp. Med. *218*, e20202617.

106. Poon, M.M.L., Rybkina, K., Kato, Y., Kubota, M., Matsumoto, R., Bloom, N.I., Zhang, Z., Hastie, K.M., Grifoni, A., Weiskopf, D., et al. (2021). SARS-CoV-2 infection generates tissue-localized immunological memory in humans. Sci. Immunol. *6*, eabl9105.

107. Wijeyesinghe, S., Beura, L.K., Pierson, M.J., Stolley, J.M., Adam, O.A., Ruscher, R., Steinert, E.M., Rosato, P.C., Vezys, V., and Masopust, D. (2021). Expansible residence decentralizes immune homeostasis. Nature *592*, 457–462.

108. Fonseca, R., Beura, L.K., Quarnstrom, C.F., Ghoneim, H.E., Fan, Y., Zebley, C.C., Scott, M.C., Fares-Frederickson, N.J., Wijeyesinghe, S., Thompson, E.A., et al. (2020). Developmental plasticity allows outside-in immune re- sponses by resident memory T cells. Nat. Immunol. *21*, 412–421.

109. Stolley, J.M., Johnston, T.S., Soerens, A.G., Beura, L.K., Rosato, P.C., Joag, V., Wijeyesinghe, S.P., Langlois, R.A., Osum, K.C., Mitchell, J.S., and Masopust, D. (2020). Retrograde migration supplies resident memory T cells to lung-draining LN after influenza infection. J. Exp. Med. *217*, e20192197.

110. Klicznik, M.M., Morawski, P.A., Ho¨llbacher, B., Varkhande, S.R., Motley, S.J., Kuri-Cervantes, L., Goodwin, E., Rosenblum, M.D., Long, S.A., Brachtl, G., et al. (2019). Human CD4+CD103+ cutaneous resident memory T cells are found in the circulation of healthy individuals. Sci. Immunol. *4*, eaav8995.

111. De Waal Malefyt, R., Abrams, J., Bennett, B., Figdor, C.G., and de Vries, J.E. (1991). Interleukin 10 (IL-10) inhibits cytokine synthesis by human monocytes: an autoregulatory role of IL-10 produced by monocytes. J. Exp. Med. *174*, 1209–1220.

112. Gazzinelli, R.T., Wysocka, M., Hieny, S., Scharton-Kersten, T., Cheever, A., Ku¨hn, R., Mu¨ller, W., Trinchieri, G., and Sher, A. (1996). In the absence of endogenous IL-10, mice acutely infected with Toxoplasma gondii succumb to a lethal immune response dependent on CD4+ T cells and accompanied by overproduction of IL-12, IFN-gamma and TNF-alpha. J. Immunol. *157*, 798–805.

113. Hunter, C.A., Ellis-Neyes, L.A., Slifer, T., Kanaly, S., Griinig, G., Fort, M., Ren- nick, D., and Araujot, F.G. (1997). 1L-10 is required to prevent immune hyper- activity During infection with Trypanosoma cruzi. J. Immunol. *158*, 3311–3316.

114. Zens, K.D., J.K. Chen, and D.L. Farber. 2016. Vaccine-generated lung tissue- resident memory T cells provide heterosubtypic protection to influenza infection. JCI Insight. 1:e85832. https://doi.org/10.1172/jci.insight.85832

115. Mackay, L.K., M. Minnich, N.A. Kragten, Y. Liao, B. Nota, C. Seillet, A. Zaid, K. Man, S. Preston, D. Freestone, et al. 2016. Hobit and Blimp1 instruct a universal transcriptional program of tissue residency in lymphocytes. Science. 352:459–463. https://doi.org/10.1126/science.aad2035

116. Slütter, B., N. Van Braeckel-Budimir, G. Abboud, S.M. Varga, S. Salek-Ar- dakani, and J.T. Harty. 2017. Dynamics of influenza-induced lung-resident memory T cells underlie waning heterosubtypic immunity. Sci. Immunol. 2:eaag2031. https://doi.org/10.1126/sciimmunol.aag2031

117. Uddba¨ck, I., E.K. Cartwright, A.S. Schøller, A.N. Wein, S.L. Hayward, J. Lobby, S. Takamura, A.R. Thomsen, J.E. Kohlmeier, and J.P. Christensen. 2020. Long-term maintenance of lung resident memory T cells is mediated by persistent antigen. Mucosal Immunol. 14(1):92–99. https://doi.org/10 .1038/s41385-020-0309-3

118. Liang, S., K. Mozdzanowska, G. Palladino, and W. Gerhard. 1994. Hetero- subtypic immunity to influenza type A virus in mice. Effector mecha- nisms and their longevity. J. Immunol. 152:1653–1661.